PREDICTION OF FREE TURBULENT MIXING USING A TURBULENT KINETIC ENERGY METHOD*

By Philip T. Harsha
ARO, Inc.

SUMMARY

Free turbulent mixing of two-dimensional and axisymmetric one- and two-stream flows is analyzed by a relatively simple turbulent kinetic energy method. This method incorporates a linear relationship between the turbulent shear stress and the turbulent kinetic energy and an algebraic relationship for the length scale appearing in the turbulent kinetic energy equation. Good results are obtained for a wide variety of flows. The technique is shown to be especially applicable to flows with heat and mass transfer, for which nonunity Prandtl and Schmidt numbers may be assumed.

INTRODUCTION

For some years a continuing research project has been underway at the Arnold Engineering Development Center (AEDC) aimed at the development of efficient and accurate techniques for the prediction of the entire range of free turbulent mixing phenomena. The goal of this project, sponsored by the Air Force Office of Scientific Research, has been the development of a method which will allow the accurate determination of the mean flow structure of free mixing flows. Although the requirements of accuracy and reliability have dictated the choice of a history-dependent model (i.e., one which takes into account some aspects of the turbulence structure), the prediction of turbulence structure per se has not been considered to be of great importance. In any event, it would seem to be unlikely that a model which predicted the mean flow field correctly for a variety of different flows, would be grossly in error in its prediction of the important features of the turbulence structure.

The model to be described in this paper is a development of the turbulent kinetic energy method originally reported by Lee and Harsha (ref. 1) and further

*This research was performed under the provisions of United States Air Force Contract No. F40600-72-C-0003 with ARO, Inc., the operating contractor of the Arnold Engineering Development Center (AEDC) for the Air Force Systems Command. Major financial support was provided by the Air Force Office of Scientific Research under Air Force Project 9711. Project Monitor was Dr. B. T. Wolfson.

described and extended to more complex flows in other publications (refs. 2 to 4). Even though the model includes flow history through its use of the turbulent kinetic energy equation, it is still an empirical model as are all current approaches to the prediction of free turbulent mixing. Indeed, the only basic difference between approaches is in the point at which empiricism enters. But although empirical information is used in this model, one restriction not commonly made is enforced: there must exist some systematic method for the application of the empiricisms to the calculation of any given flow. Put another way, the empiricisms must either be universal or have clearly defined limits of validity.

It is perhaps important to introduce the analytical model to be described in this paper with a summary of the features of the basic work described in references 1 to 4. In the first of these papers (ref. 1) a simple turbulent kinetic energy model was introduced, in which a linear relation between the turbulent kinetic energy and turbulent shear stress was employed to obtain the shear stress from the solution of the turbulent kinetic energy equation. Gradient diffusion of turbulent kinetic energy was assumed with a constant "kinetic energy Prandtl number," and the length scale required to evaluate the dissipation term in the kinetic energy equation was taken to be proportional to the local width scale of the mixing zone. In this context the model introduced and applied to two simple flows in reference 1 is a single-equation model, since compared to an eddy viscosity method, the only additional equation required is the turbulent kinetic energy equation. Universal constants were assumed for the kinetic energy Prandtl number, for the ratio between turbulent shear stress and turbulent kinetic energy, and in the dissipation term.

The work described in reference 2 (summarized in ref. 3) and the similar work described in reference 4 involved the application of the method to progressively more complex free mixing flows, including flows with heat and mass transfer. Throughout this work the universal constants defined in reference 1 were retained. In reference 2, which to some extent parallels the approach of this conference, the predictions of this single-equation turbulent kinetic energy method were compared with the predictions of a number of eddy viscosity models for a wide variety of flows, including several that are included as test cases for this conference. The conclusion drawn from this comparison was that, even though some serious difficulties remained, the predictions of the turbulent kinetic energy model with the universal constants were, in general, better than those of any eddy viscosity model tested when it was required that the constants appearing in the eddy viscosity models also be considered to be universal.

In particular, good agreement between kinetic energy theory and experiment was shown in reference 2 for coaxial air-air mixing, similar to test cases 9 and 20 of this conference, for hydrogen-air mixing, similar to test cases 10 and 21, and for wake flows such as test cases 14 and 15. Indeed, based on the work of reference 2, it is clear that the universal constant model would be capable of predicting at least 8 and probably 10 of

the 23 available test cases for this conference without change. However, reference 2 also showed that the universal-constant model was clearly in error for the important jet into still air flows. In addition, the asymptotic two-dimensional shear layer had not been attempted nor had initial conditions other than experimental shear stress profiles been used, except for one flow. Inevitably, the extension of the model described in references 1 to 4 to handle such problems led to the need for refinement of some features of the model.

As might be expected, the refinements incorporated in the model described in this paper involve the empirical functions that must be introduced to close the turbulent kinetic energy equation. The new functions have been developed primarily through a process of computer experimentation, in which the predictions made by turbulent kinetic energy theory have been compared both with experimental data and with the predictions of simple eddy viscosity models in those flows in which the simple models are known to be adequate. The integral turbulent kinetic energy theory developed by C. E. Peters at AEDC, which is briefly described in paper no. 17 of this compilation, has been very useful in the development of these improved functions. Such a theory allows a rapid investigation of the asymptotic behavior of a given turbulent kinetic energy model in certain relatively simple flows without the numerical complications that can develop with finite-difference techniques. In addition, integral techniques, in which the profiles of the dependent variables are specified a priori, eliminate the problem of specification of a diffusion function for turbulent kinetic energy (since the lateral diffusion integrated over a profile at a given x must be zero) and allow the production and dissipation terms to be evaluated in terms of integral quantities. This then simplifies the interpretation of the effects of changing the constants appearing in the turbulent kinetic energy equation for flows in which the profiles of the dependent variables can be adequately prescribed.

SYMBOLS

a_1 ratio of turbulent shear stress to turbulent kinetic energy, $\tau/\rho k$

a_2 dissipation parameter (see eq. (1))

b local width of mixing region

c jet species concentration

D diameter

k turbulent kinetic energy per unit mass, $1/2\left(\overline{u'^2 + v'^2 + w'^2}\right)$

k_p constant in Prandtl exchange coefficient model

l_k length scale, equal to distance between $0.90\Delta u$ and $0.10\Delta u$ in a shear layer, distance between $0.99\Delta u$ and $0.01\Delta u$ in the core region of a jet, and $2r_{1/2}$ in an axisymmetric flow

M Mach number

Pr_k kinetic energy Prandtl number

Pr_T turbulent Prandtl number

R_T "turbulent Reynolds number," equation (2)

r radius

Sc_T turbulent Schmidt number

T static temperature

u velocity

Δu characteristic velocity difference, $\left(u_{max} - u_{min}\right)$

$\overline{u'v'}$ turbulent shear stress correlation

v mean-flow lateral velocity component

$W = 1 - \frac{u_c}{u_e}$

x axial coordinate

y general lateral coordinate

α concentration

β parameter, 1 for axisymmetric flow and 0 for two-dimensional flow

δ_o initial boundary-layer thickness

ϵ turbulent eddy viscosity, $\frac{\tau/\rho}{\partial u/\partial y}$

θ momentum thickness

ρ density

σ_o reference value of spreading parameter σ

τ turbulent shear stress, $-\rho\overline{u'v'}$

Subscripts:

c center-line value

e free-stream value or maximum value in outer jet for coaxial mixing

max maximum value at cross section

min minimum value at cross section

o value at the nozzle

1 value on high velocity side of shear layer

2 value on low velocity side of shear layer

1/2 or mu value at point at which $u = 1/2(u_c + u_e)$

ANALYSIS

In addition to the continuity, momentum (mean flow), energy, and species equations necessary in any treatment of a general free turbulent mixing problem, the method described in this paper involves the solution of the turbulent kinetic energy equation. This equation can be written as described, for example, in reference 2: The parameter β is 0 for a two-dimensional flow and 1 for an axisymmetric flow.

$$\underbrace{\rho u \frac{\partial k}{\partial x} + \rho v \frac{\partial k}{\partial y}}_{\text{Convection}} = \underbrace{\frac{1}{y^\beta}\frac{\partial}{\partial y}\left(\frac{\rho \epsilon y^\beta}{Pr_k}\frac{\partial k}{\partial y}\right)}_{\text{Diffusion}} + \underbrace{\tau \frac{\partial u}{\partial y}}_{\text{Production}} - \underbrace{\frac{a_2 \rho k^{3/2}}{l_k}}_{\text{Dissipation}} \qquad (1)$$

In the development of this equation and its application along with the momentum equation to the solution of a given problem, empirical hypotheses have been invoked at three points. The first of these is in the definition of the appropriate form for the diffusion of turbulent kinetic energy. Equation (1) incorporates a gradient diffusion hypothesis; such a hypothesis, with a constant "kinetic energy Prandtl number" Pr_k equal to 0.70, was used in the model described in references 1 to 4, and is also used in this paper.

As written in equation (1), the form assumed for the dissipation term is unchanged from the earlier work. However, whereas a universal constant value for a_2, equal to 1.5, was assumed in the earlier work, constant a_2 fails to yield the proper asymptotic behavior in all flows, and an expression allowing axial variation of a_2 has been developed. No lateral variation of a_2 is allowed.

The third hypothesis is the relation between turbulent shear stress and turbulent kinetic energy. Again, the form of the relationship is the same as that used previously:

$$\tau = a_1 \rho k$$

In the earlier work, two expressions for the lateral variation of a_1 have been used. For two-dimensional flows (including the core region of an axisymmetric jet), a_1 has been taken to be essentially constant, with a value of 0.3 (and with its sign defined by the velocity gradient), whereas in axisymmetric flow, the expression

$$a_1 = \frac{0.3(\partial u/\partial r)}{\left|\partial u/\partial r\right|_{max}}$$

has been shown to apply (ref. 3). However, in the course of the work described in this paper, it became clear that a new function for the lateral variation of a_1 had to be developed for the two-dimensional shear layer. Such a function was devised and is described subsequently; the new function also has certain implications for the prediction of the core region of axisymmetric jets.

In addition, one of the often mentioned problems with turbulent kinetic energy methods is the fact that at the initial station, turbulent shear stress profiles are needed, and experimental profiles are seldom available. In the work described herein, two simple techniques have been used to start the calculations, the choice depending on the position of the start profile. Neither of these techniques involves a detailed knowledge of the initial shear stress profiles. Taken together, they effectively remove the "initial shear stress profile" objections.

The Dissipation Function

As mentioned previously, it quickly became evident during the development of the integral turbulent kinetic energy theory by C. E. Peters and W. J. Phares (paper no. 17) that a constant value of a_2 could not provide the proper asymptotic behavior for all flows considered in this conference. Although it is certainly arguable that the reason for this lies in the form of the term itself, it is less complicated to obtain the proper asymptotic behavior through variation of a_2, if this is at all possible. Thus, the basic $k^{3/2}/l_k$ proportionality has been formally retained, with a new expression describing the axial variation of a_2.

The a_2 function developed by Peters is based on a "turbulent Reynolds number" R_T defined as

$$R_T = \frac{\Delta u l_k}{\epsilon} \tag{2}$$

where Δu is a characteristic velocity difference across the mixing region, such as $u_{max} - u_{min}$; l_k is a characteristic length scale, for example, twice the half-velocity width $r_{1/2}$ in an axisymmetric flow; and ϵ is the local value of the effective (or eddy) viscosity. Because Peters evaluates the shear stress at only one point in a lateral profile $y_{1/2}$, R_T needs only one value at a given x; in the present work R_T varies across a profile, but in order to assign a characteristic value, the point of maximum turbulent energy is chosen as the point to evaluate R_T. With R_T defined as in equation (2), the appropriate values of this parameter can be immediately written down for some flows for which the Prandtl eddy viscosity model

$$\epsilon = k_p l_k \Delta u = \frac{1}{R_T} l_k \Delta u$$

is known to provide a good asymptotic prediction. Thus, for the incompressible two-dimensional shear layer, for which $k_p = 0.007$, R_T is 143, whereas for a circular jet in still surroundings, for which $k_p = 0.0125$, R_T is 80.

The relation between a_2 and R_T used in this work is one of a family of relations developed by Peters and is given by

$$a_2 = 3.89 - \frac{315}{R_T} \qquad (R_T > 143) \tag{3a}$$

$$a_2 = 1.69 \qquad (70 < R_T < 143) \tag{3b}$$

$$a_2 = 0.99 + 0.01R_T \qquad (R_T < 70) \qquad (3c)$$

The relationship expressed by equations (3) is not entirely optimum for the calculations described in this paper, primarily, because of differences in the point in a lateral profile at which R_T is calculated between the integral and the finite-difference methods. In particular, the point at which equation (3c) is applied in the finite-difference method probably should be at $R_T < 30$, and the break at $R_T = 143$ needs to be handled more gradually than equations (3) allow. However, as the results will show, equations (3) do allow the accurate calculation of a very wide variety of flows. Further development of the empirical functions represented by equations (3) is continuing; some of this development is described by Peters in paper no. 17.

Relation Between Shear Stress and Kinetic Energy

Although a_1, the ratio of the turbulent shear stress to the turbulent kinetic energy, is sensibly constant (at a value of 0.3) for a wide variety of flows (ref. 5), the necessity of allowing for some lateral variation of a_1 has always been understood. Thus, in previously reported work in axisymmetric flow, the expression

$$a_1 = \frac{0.3(\partial u/\partial r)}{|\partial u/\partial r|_{max}}$$

(where the subscript "max" refers to the point where $\partial u/\partial r$ attains its maximum value) has been used from the center line to the point at which

$$\frac{\partial u}{\partial r} = \left(\frac{\partial u}{\partial r}\right)_{max}$$

with the expression

$$a_1 = \frac{0.3(\partial u/\partial r)}{|\partial u/\partial r|}$$

being used for the rest of the profile to insure the proper algebraic sign for the shear stress. In two-dimensional flow, the expression

$$a_1 = \frac{0.3(\partial u/\partial y)}{|\partial u/\partial y|_{max}}$$

was used only in a small region around the point of maximum or minimum velocity gradient, primarily to avoid excessive steepening of this gradient.

However, in the course of the work carried out for this paper, it was found to be impossible to obtain an accurate prediction of the incompressible two-dimensional shear layer by using either of the two models described previously. Because the problem lay in the prediction of shear stress at the profile edge, it was not possible to determine the appropriate a_1 function from comparison with experimental data. Instead, use was made of the fact that the incompressible two-dimensional shear layer is one of the flows for which the Prandtl eddy viscosity model provides an accurate asymptotic prediction. A calculation was made with the Prandtl model to obtain the shear stress and the production term in the turbulent kinetic energy equation. The resulting shear stress and kinetic energy profiles were then used to obtain the lateral variation of the parameter a_1, as shown in figure 1. In this figure, the symbols represent different x-locations at which the calculated profiles were obtained, and the solid line represents the a_1 function derived from these results. Positive values of the abscissa represent the high-velocity edge of the shear layer. This variation was found to be reasonably universal for the incompressible shear layer, as can be seen from the figure, and has been used in all asymptotic shear layer calculations in this study.

The a_1 profile obtained for the two-dimensional shear layer may also be appropriate for the mixing layer in the core region of a jet. Because of time limitations it has not been possible to investigate the application of the a_1 function to these flows, but it is possible that use of a function such as that represented by figure 1 will reduce the fairly long transition region that is predicted in some of the flows described in the following section.

Initial Conditions

The most often-quoted major objection to the use of turbulent energy methods in the prediction of free turbulent mixing has been the apparent necessity of obtaining a turbulent shear stress (or turbulent kinetic energy) profile to start the calculation. In the calculations described, this problem has been in large part overcome; experimental shear stress profiles have not been used to start any of the calculations reported herein, and experimental estimates of the turbulent shear stress level have been used in only those few cases where other estimates could not properly be made.

To start these calculations, two techniques have been used. In all cases in which the initial profiles have been given at $x = 0$, the turbulent eddy viscosity profiles obtained for boundary-layer flows by Maise and McDonald (ref. 6) have been used to obtain the profiles of the turbulent shear stress. These profiles were also used for the boundary-layer portion of the initial velocity profile for the compressible two-dimensional shear layer (test case 5), although the start point for this case was not at $x = 0$. In all other computations, for which profiles have been given downstream of the origin of mixing (usually in the core region of a jet flow), constant eddy viscosity has been used to generate the initial shear stress profile. One exception is test case 24, for which the start point was in the laminar part of the flow. The eddy viscosity has in general been that appropriate for $R_T = 200$ (i.e., a Prandtl constant of 0.005), although in a few cases a more accurate estimate of the experimental R_T was necessary. As the results described in the next section show, it is not necessary to have detailed knowledge of the initial shear stress distribution for each case in order to get accurate predictions of the flow development.

Numerical Solution Technique

The finite-difference numerical technique used to make the calculations reported herein is identical to that reported in references 1 to 4. One of the features of this technique is that the constant-momentum-excess requirement applicable to free turbulent flows is satisfied at each station; that is,

$$\int_0^\infty \rho u(u - u_e)y^\beta dy = \text{Constant}$$

As a cross-check, the value of the product $\left(r_{1/2}/r_o\right)\left(u_c/u_o\right)$ was evaluated for the axisymmetric jet flow of test case 18. If momentum is conserved, this product should be constant for the similar profile region of the flow. Over the range $30 < x/D < 115$, the value of $\left(r_{1/2}/r_o\right)\left(u_c/u_o\right)$ varied within ±1.5 percent of its average for this calculation.

RESULTS

Successful computations were completed for 23 of the 24 test cases that were available. The only case not computed was test case 23, the compound coaxial jet, which would have required fairly complicated reprograming to account for the simultaneous development of two shear layers.

Because of the large number of cases to be covered, the discussion in this section is limited to the most significant aspects of each case computed. The comments to follow in the main emphasize the problems encountered in these computations. The overall

success of the method described in this paper will speak for itself. General details of the starting techniques and the dissipation function used are noted in table I, which also provides a guide to the appropriate figures.

Two-Dimensional Shear Layers

As might be inferred from the discussion of the a_1 function, the five shear layer cases required a relatively large development effort which is not yet complete. This development effort was particularly important for the three asymptotic cases, for which the new a_1 function was particularly necessary. For test cases 1 to 3, the calculations began with initial shear stress profiles obtained from the appropriate Maise and McDonald eddy viscosity profiles (ref. 6) and constant a_1, as is appropriate for boundary-layer flow. At an arbitrary distance downstream the a_1 profile indicated in figure 1 was introduced (approximated analytically by a series of straight-line segments). For test cases 1 to 3, since only the asymptotic behavior was required, the point at which the new a_1 function was applied could be truly arbitrary (it was taken to be 1 initial boundary-layer height), but as will be seen in test cases 4 and 5, the choice can be important for the preasymptotic shear layer. No transition function was used to change from a constant a_1 profile to the profile shown in figure 1.

Self-preservation was approached at relatively small axial distances for the incompressible shear layers, although with values of σ lower than are commonly reported. The calculation of σ was made by using the standard definition of σ for this conference

$$\sigma = 1.855 \frac{x_2 - x_1}{y_2 - y_1}$$

where y_1 and y_2 represent the lateral distance between the points at which $\frac{u - u_2}{u_1 - u_2} = 0.1$ and $\frac{u - u_2}{u_1 - u_2} = 0.9$ at x_1 and x_2, respectively. Figure 2 shows that the profile shape passes through a shape appropriate to the $\sigma = 11.8$ data of Liepmann and Laufer (ref. 7), but at these distances it is apparently still evolving with σ decreasing. Figure 3 shows that the predictions of σ are apparently uniformly low, since the classical behavior of σ with velocity ratio is recovered.

There is no evidence that the a_1 profile represented in figure 1 is invariant either with Mach number variation or density ratio variation. Indeed, there is some evidence that it is not, primarily from the differences between these calculations and those reported by Peters and Phares (paper no. 17). In the latter work, the shape of the turbulent kinetic energy profile is assumed to be invariant, which implies that the lateral variation of the

ratio of the turbulent shear stress to the turbulent kinetic energy (i.e., a_1) cannot be invariant with either Mach number or density ratio variation. In any event, the a_1 function shown in figure 1 was used for all shear layer calculations, and figure 4 shows the predicted variation of σ with Mach number. Note particularly the extremely great distances required to approach a self-preserving condition at the higher Mach number.

The variation of σ with density ratio predicted by using this model is shown in figures 5 and 6. As noted in figure 6, the density ratio was obtained by varying the temperature of the two streams. Within the framework of the commonly made unity turbulent Lewis number assumption, similar results would be obtained by varying the molecular weight of the two streams. However, the unity turbulent Lewis number assumption is not necessary in the analysis. The predicted variation of σ with density ratio is completely different from that predicted for a similar variation in density ratio caused by Mach number variation.

The asymptotic two-dimensional shear layer predictions are not meant to represent an adequate and correct theory of this particular flow. They do show the necessity for including a different sort of lateral variation of a_1 in such a flow from that which is necessary in other flows. This lateral variation may in turn be important in the prediction of the core region of axisymmetric jets. Further, these calculations indicate that, at least in some instances, self-preservation is only very slowly reached – an observation that raises obvious questions about the interpretation of experimental results.

Self-preservation, or the lack of it, is also a factor in the two remaining shear layer flows, test cases 4 and 5. In these calculations direct comparison with experimental profile data is made, and these comparisons indicate that both of these flows were preasymptotic.

Evidence for this statement in test case 4 is shown in figure 7, which shows that the "constant a_1" model provides a better prediction of the velocity profile at $x = 76$ cm than does the "shear layer a_1" model. For both test case 4 and test case 5, the predicted profiles were matched with the experimental ones at the half-velocity points. This technique was necessary because the calculation does not satisfy the proper lateral boundary condition at plus or minus infinity. As is well known, the effect of neglect of this boundary condition is to allow the calculated profiles to "float" in space.

The comparison of shear stress profiles for test case 4 shown in figure 8 shows that the constant a_1 model overpredicts the shear stress at $x = 12.7$ cm and strongly underpredicts it at $x = 76$ cm. However, analysis of the shear stress profiles given for test case 4 shows that the peak shear at $x = 76$ cm is considerably higher than the trend from the upstream data would indicate it should be. (The experimental peak shear stress is almost constant at $x = 25$ cm and $x = 46$ cm.) Furthermore, it is unlikely that an error in shear stress prediction of the magnitude shown in figure 8 at $x = 76$ cm would

be reflected by the small velocity profile deviations shown in figure 7 at this station. Therefore, the reported value of shear stress at $x = 76$ cm is, in the author's opinion, suspect.

Test case 5 is also evidently preasymptotic, as the comparison of the experimental and predicted velocity profiles in figure 9 shows. Again, the constant a_1 model provides the better prediction. This test case and test case 4 both raise the question of what is the proper point to begin to use the "asymptotic" a_1 profile represented by figure 1. The answer to this question clearly requires further research.

Axisymmetric Jets Into Still Air

Three test cases in the category of axisymmetric jets into still air were considered, test cases 6 to 8, and the results were good for all cases as figures 10 to 13 demonstrate. For all these calculations, the constant a_1 model was used in the mixing layer region (first regime) of the flow. Downstream of the end of the potential core, the model in which the constant value of a_1 is modified by the velocity gradient ratio was used as was used for all axisymmetric flows. The point at which the change of models takes place is arbitrarily assumed to be that at which the center-line velocity is 0.9 times the jet velocity. No transition function was used.

The prediction of the subsonic jet of test case 6 began at $x/r_o = 2$ with a Prandtl constant $k_p = 0.005$. As can be seen from figure 10, the prediction of this flow is quite good. The fact that the prediction is better if equation (3c) is not used, despite the fact that the predicted asymptotic value of the turbulent Reynolds number R_T is 35, indicates that for these predictions, the upper limit for the use of equation (3c) should be reduced.

One point of difference between this calculation and the integral technique reported by Peters is that the R_T value is in this analysis obtained at the point at which $k = k_{max}$ rather than the half-velocity point. This tends to lower the value of R_T somewhat compared with the value obtained by Peters. It would also have been possible in this analysis to evaluate R_T at the point at which $\tau = \tau_{max}$, which does not in general correspond to the point at which $k = k_{max}$. Had this been done, there would have been a 10-percent increase in R_T for the air-air flows, for which the eddy viscosity is essentially constant over the inner portion of the flow, and perhaps a 40-percent increase in R_T for hydrogen-air flows. Thus, the point at which R_T is evaluated is only a substantial factor in hydrogen-air flows for which the upper limit for equation (3c) is not a factor.

For test case 7, the length of the potential core is somewhat underpredicted, resulting in an overall overprediction of the velocity decay, as shown by figure 11. On the other hand, the profile prediction is quite good (fig. 12) if the underprediction of the center-line velocity is taken into account. The profile data are from reference 8.

Finally, the excellent center-line temperature and velocity agreement with the data of test case 8 (fig. 13) is obtained by using an assumed (and constant) value of 0.85 for the turbulent Prandtl number.

Jets in Moving Streams

The first of the coaxial jet cases, test case 9, represents the data of Forstall (ref. 9). For these calculations, the 10 percent by volume helium trace was included so that the initial jet to outer stream density ratio was 0.92. In table I it is noted that two initial profile offsets were used in the calculation for test case 9. One calculation was made by using the shifted profiles given by the data sheet for test case 9, and the others were made by using the unshifted profiles given in the data sheet. Figure 14 demonstrates that the most accurate prediction uses the latter start condition and further neglects the use of equation (3c). The initial radii reported in figure 14 represent the location of the inner edge of the viscous region. For test case 9, as for test case 6, the asymptotic value of R_T is of the order of 35, indicating again that the upper limit for equation (3c) should be of the order of $R_T = 30$ for this method. Profiles of velocity and concentration are shown in figure 15 (the data obtained from curves presented in ref. 9), and figure 16 shows excellent agreement with the data for the half-velocity width calculation. Both of these figures relate to the "unshifted" calculation shown by the dashed line in figure 14, for which equation (3c) is not used.

Perhaps the strongest feature of the method described in this paper is the relative ease and accuracy with which more complex flows involving heat and mass transfer are handled. Figures 17 and 18 show the excellent agreement between theory and experiment for the hydrogen-air mixing data of test case 10. The experimental profile data were obtained from reference 10.

For test case 10 (and the similar data of test case 21) a second regime start point was assumed for the calculations; that is, the initial viscous region was assumed to extend all the way to the center line. The profile data were obtained, as in all the calculations, from the appropriate data sheet. The start points for both test cases 10 and 21 are in the transition region between the first and second flow regimes, and such start points are among the most difficult to use with this method. For calculations which start at $x/D = 0$, the natural tendency is for the level of kinetic energy near the inside edge of the viscous region to increase fairly slowly but rapidly enough that the center-line kinetic energy is of the order of 70 percent of the maximum in a profile at the point at which the "second regime" a_1 profile is put into effect. In calculations starting in the transition region as this one does, the increase in kinetic energy near the inside edge of the viscous region does not occur, so that the kinetic energy (and hence the shear stress) is too low near the flow center line. The result is an excessively long transition region, with

6 diameters being required in this particular flow for the center-line velocity ratio to drop to 0.90.

However, this problem was overcome within the framework of a constant eddy viscosity start profile by using the second regime velocity gradient ratio throughout the flow. Since the initial shear stress is input, the initial kinetic energy was obtained by using the second regime velocity gradient ratio inverted; thus, the initial kinetic energy was maintained at a constant value from the center line to the maximum velocity gradient point, which is a reasonable approximation to the form that the kinetic energy profile would have had if the calculation started at $x = 0$. It must be stressed that this is only a problem if a transition region start is used and, thus, was only a problem for test cases 10 and 21. The hydrogen-air flows of test cases 12 and 22 did not require such treatment.

Incidentally, the value of the Prandtl constant implied by the shear stress used to start this calculation, which was obtained from the τ_{mu} data of reference 10, and the assumed width of the profile, is $k_p = 0.005$, the same as has been generally assumed for nonzero start points.

The data of test case 11 have some curious features, not the least of which is the fact that the value of the center-line velocity, initially lower than the free-stream velocity, drops still lower before beginning to rise. Nevertheless, the overall prediction still compares favorably with the data as shown in figure 19.

Comparison of the theoretical prediction of test case 12 with the experimental data (fig. 20) indicates that very good results can be obtained for hydrogen-air flow with a calculation starting at $x/D = 0$, with a Maise and McDonald eddy viscosity profile being used to obtain the initial shear stress. Profile comparison (fig. 21) also shows reasonably good agreement, if the difference between the predicted and actual center-line values at the axial station chosen is taken into account. The data are from reference 11.

The prediction of the two-dimensional jet in a moving stream, test case 13, is shown in figure 22. For this case, no initial boundary-layer data other than an initial momentum thickness for the two boundary layers together were available. Calculations were begun with 1/4 power-law initial boundary-layer profiles because the 1/7 power-law profile ordinarily used resulted in extremely thick initial boundary layers being necessary to equal the quoted momentum thickness. Maise and McDonald eddy viscosity profiles were used to obtain the initial shear stress level. The agreement between the experimental values of center-line velocity and the computed values is quite good as can be seen from figure 22.

Wakes

Accurate prediction of the two-dimensional wake flows required the use of a constant value of a_2 rather than the variation described by equations (3). The value 1.4 was considerably lower than equations (3) would predict at the R_T appropriate to the flow. For axisymmetric values, the function described by equations (3) seems to be adequate. However, the prediction of the axisymmetric wake flows is not sufficiently good for any strong conclusions to be drawn regarding the optimum a_2 for those flows.

The center-line velocity prediction for a preasymptotic two-dimensional wake, case 14, is shown in figure 23. Because the presentation method tends to emphasize the discrepancies between theory and experiment rather markedly, velocity profile shapes are compared in figure 24. The corresponding turbulent shear stress profiles are shown in figure 25, which indicate that the Maise and McDonald eddy viscosity profiles used to start these calculations may have significantly underpredicted the actual initial shear stress level.

Theory and experiment for an axisymmetric wake, test case 15, are compared in figure 26.

The asymptotic two-dimensional wake data of test case 16 were computed by using the initial R_T reported in reference 12 to obtain the initial shear stress. Prediction and experiment are compared in figure 27.

Again, an initial R_T reported in reference 12 was used to start the computation for test case 17, an axisymmetric wake; the comparison between theory and experiment is shown in figure 28.

Optional Test Cases

The first of the optional cases, test case 18, is the prediction of the asymptotic free jet. Unfortunately, the data given are not appropriate for an asymptotic jet. Figure 29 shows the center-line velocity decay for the data of reference 13 from which test case 18 was taken; it can be seen that the prediction for this case goes essentially through the data points. The start condition was taken from the data of Bradshaw, Ferriss, and Johnson (ref. 14) at $x/D = 1$. Also shown in figure 29 are the free jet center-line velocity results obtained by Albertson, Dai, Jensen, and Rouse (ref. 15), which follow the classical $(x/D)^{-1}$ decay law quite well. Clearly, the data of reference 13 do not satisfy this decay law, and, for $x = 100$, the center-line velocity recorded by Wygnanski and Fiedler (ref. 13) is considerably lower than that which would be obtained from an $(x/D)^{-1}$ decay from, say, $x/D = 40$. For a free jet, the excess momentum integral must be a constant. Thus, if two flows vary in center-line velocity with constant momentum excess in such a manner that the center-line decay curves cross, one would expect the flow with the lower center-line velocity to have the wider profile. Comparing the test case 18 data with data

from reference 15 (fig. 30) shows that this is not true. On the other hand, the theory does show a wider profile than either the reference 15 data or the test case 18 data. Therefore, the conclusion is made that the data for test case 18 were not, in fact, properly asymptotic.

Figure 31 demonstrates the good agreement of the present method with the data of test case 19. Three further coaxial mixing cases are presented in figures 32 to 36. Note especially the excellent profile agreement shown in figures 33 and 35, along with the good axial decay agreement shown in figures 32 and 34 for both test cases 20 and 21. Figure 36 demonstrates the quite acceptable prediction of the unusual hydrogen-air flow of test case 22 achieved with the present method. This method will, of course, not predict the negative velocity ratios measured experimentally, and the computation stopped at $x/D = 26$ where the velocity profile had all but flattened out.

The last case to be discussed is the interesting two-dimensional wake flow of test case 24. The start point for this case is in the laminar portion of the flow; there follows in the experimental data a fairly long transition region until behavior characteristic of a turbulent flow develops. In the computation of this flow, the viscosity term appearing in the momentum equation was taken to be made up of a laminar and a turbulent contribution. The laminar contribution was obtained from the experimental data of reference 12, and the turbulent contribution was obtained through the solution of the turbulent kinetic energy equation in the normal manner. A very low, uniform, initial turbulent kinetic energy profile was used to provide the initial condition for the solution of the turbulent kinetic energy equation, and the level of the energy was allowed to develop as described by the equation. Referring to the turbulent kinetic energy equation (eq. (1)), the production term was evaluated with only the turbulent contribution to the shear stress, whereas the viscosity appearing in the diffusion term was taken to be the total viscosity.

Results of several computations with this approach are shown in figure 37. The computations differ only in the initial turbulent kinetic energy level assumed. This level is described in the figure in terms of the associated turbulent intensity level based on an assumed isotropic condition – that is, $u' = v' = w'$. As can be seen from the figure, the effect of increasing the initial intensity level is to shorten the transition region, as would be expected. Note also that the level giving the best agreement with the data is 2 percent, which agrees well with the quoted intensity levels from reference 12, which, based on the outer stream mean velocity, ranged from 0.3 percent to 3 percent through the laminar and transition regions. Because the wake was heated, the turbulent Prandtl number for these calculations was taken to be 0.85.

Since it was not possible to completely establish a priori an appropriate start condition for this problem, the results shown herein should only be taken as a demonstration of the abilities of the method described in this report, using an admittedly crude start

technique. Transitioning flows such as test case 24 would appear to require more knowledge of the experimental initial conditions than fully turbulent flows.

CONCLUDING REMARKS

As was stated in the introduction, the work described in AEDC-TR-71-36 made it clear that the universal constant kinetic energy approach described in that reference was capable of handling a substantial number of the test cases for this conference without change. Indeed, ignoring the free shear layer cases for the moment, the only obvious area in which this method would have clearly failed was in the prediction of the circular jet, test cases 6, 7, 8, 18, and 19. On the other hand, it had not been developed to the point that calculations could be routinely initiated without detailed knowledge of the initial shear stress profiles.

The results described in this paper show that with a small increase in complexity – that is, the addition of a function describing the axial variation of the dissipation parameter a_2 – the kinetic energy method described in AEDC-TR-71-36 can be applied to a wide variety of flows of engineering interest. In particular, accurate predictions of jets with zero secondary flow and coaxial jets, including heat and mass transfer, can routinely be made without exact knowledge of the initial shear stress profiles and with a well-defined method of obtaining the necessary empirical constants which does not involve prior knowledge of the results desired.

Some work is still required to obtain the optimum function for the dissipation parameter a_2. The asymptotic free jet prediction does not seem proper, as the classical center-line velocity decay rate is not recovered. Also, the shear layer form for the lateral variation of the ratio of shear stress to turbulent kinetic energy, a_1, needs to be further investigated, with particular emphasis on the effects of Mach number and density variation. Further work is underway on this problem, as well as on the problem of integrating the shear layer a_1 model into an overall model for better prediction of the core region of axisymmetric jets.

REFERENCES

1. Lee, S. C.; and Harsha, P. T.: Use of Turbulent Kinetic Energy in Free Mixing Studies. AIAA J., vol. 8, no. 6, June 1970, pp. 1026-1032.

2. Harsha, Philip Thomas: Free Turbulent Mixing: A Critical Evaluation of Theory and Experiment. AEDC-TR-71-36, U.S. Air Force, Feb. 1971. (Available from DDC as AD 718 956.)

3. Harsha, Philip T.: Free Turbulent Mixing: A Critical Evaluation of Theory and Experiment. Turbulent Shear Flows, AGARD-CP-93, Jan. 1972, pp. 17-1 – 17-11.

4. Harsha, P. T.; and Lee, S. C.: Analysis of Coaxial Free Mixing Using the Turbulent Kinetic Energy Method. AIAA J., vol. 9, no. 10, Oct. 1971, pp. 2063-2066.

5. Harsha, P. T.; and Lee, S. C.: Correlation Between Turbulent Shear Stress and Turbulent Kinetic Energy. AIAA J., vol. 8, no. 8, Aug. 1970, pp. 1508-1510.

6. Maise, George; and McDonald, Henry: Mixing Length and Kinematic Eddy Viscosity in a Compressible Boundary Layer. AIAA J., vol. 6, no. 1, Jan. 1968, pp. 73-80.

7. Liepmann, Hans Wolfgang; and Laufer, John: Investigations of Free Turbulent Mixing. NACA TN 1257, 1947.

8. Eggers, James M.: Velocity Profiles and Eddy Viscosity Distributions Downstream of a Mach 2.22 Nozzle Exhausting to Quiescent Air. NASA TN D-3601, 1966.

9. Forstall, Walton, Jr.: Material and Momentum Transfer in Coaxial Gas Streams. Sc.D. Thesis, Massachusetts Inst. Technol., June 1949.

10. Chriss, D. E.; and Paulk, R. A.: An Experimental Investigation of Subsonic Coaxial Free Turbulent Mixing. AEDC-TR-71-236, AFOSR-72-0237TR, U.S. Air Force, Feb. 1972. (Available from DDC as AD 737 098.)

11. Eggers, James M.: Turbulent Mixing of Coaxial Compressible Hydrogen-Air Jets. NASA TN D-6487, 1971.

12. Demetriades, A.: Compilation of Numerical Data on the Mean Flow From Compressible Turbulent Wake Experiments. Publ. No. U-4970, Aeronutronic Div., Philco-Ford Corp., Oct. 1, 1971.

13. Wygnanski, I.; and Fiedler, H.: Some Measurements in the Self-Preserving Jet. J. Fluid Mech., vol. 38, pt. 3, Sept. 18, 1969, pp. 577-612.

14. Bradshaw, P.; Ferriss, D. H.; and Johnson, R. F.: Turbulence in the Noise-Producing Region of a Circular Jet. J. Fluid Mech., vol. 19, pt. 4, Aug. 1964, pp. 591-624.

15. Albertson, M. L.; Dai, Y. B.; Jensen, R. A.; and Rouse, Hunter: Diffusion of Submerged Jets. Paper No. 2409, Trans. Amer. Soc. Civil Eng., vol. 115, 1950, pp. 643-664.

TABLE I.- SUMMARY OF CALCULATION TECHNIQUES

Test case	Type	Start point	Start method	Dissipation parameter	Figure	Remarks
1	Incompressible 2D shear layer	x = 0 cm	Maise & McDonald eddy viscosity	$a_2 = 1.69$	3	Uses a_1 profile from fig. 1
2	Compressible 2D shear layer	x = 0 cm	As for case 1	Eqs. (3)	4	As for case 1
3	Variable density 2D shear layer	x = 0 cm	As for case 1	Eqs. (3)	5, 6	As for case 1
4	Incompressible 2D shear layer	x = 0 cm	As for case 1	$a_2 = 1.69$ Eqs. (3)	7, 8	As for case 1; also with a_1 = Constant
5	Compressible 2D shear layer	x = 2.5 cm	As for case 1[a]	Eqs. (3)	9	As for case 4
6	Circular jet	x/D = 1	Prandtl ϵ, $k_p = 0.005$	Eqs. (3)	10	$a_{2,min} = 1.69$ in one calculation
7	Supersonic circular jet	x = 0 cm	Maise & McDonald eddy viscosity	Eqs. (3)	11, 12	
8	Compressible circular jet	x/D = 2.8	Prandtl ϵ, $k_p = 0.005$	Eqs. (3)	13	
9	Coaxial air jets with He trace	x/D = 0	Maise & McDonald eddy viscosity	Eqs. (3a), (3b)	14, 15, 16	Two initial profile offsets
10	Coaxial H_2-air	x/D = 3	Constant eddy viscosity	Eqs. (3)	17, 18	ϵ obtained from extrapolation τ_{mu} plots of ref. 10
11	Compressible coaxial air-air	x/D = 0	Maise & McDonald eddy viscosity	Eqs. (3a), (3b)	19	
12	Compressible coaxial H_2-air	x/D = 0	As for case 11	Eqs. (3)	20, 21	Initial velocity profile from data of ref. 14
13	Plane jets	x = 0 cm	As for case 11	Eqs. (3)	22	
14	Incompressible plane wake	x = 0 cm	Maise & McDonald eddy viscosity	$a_2 = 1.4$ (constant)	23, 24, 25	
15	Incompressible axisymmetric wake	x/D = 0	Prandtl ϵ, $k_p = 0.005$	Eqs. (3)	26	
16	Compressible plane wake	x = 0.91 cm	Constant eddy viscosity	$a_2 = 1.4$ (constant)	27	ϵ obtained from extrapolation of R_T plots of ref. 12
17	Compressible axisymmetric wake	x = 6.74 cm	Constant eddy viscosity	Eqs. (3)	28	As for case 16
18	Circular jet	x/D = 1	Prandtl ϵ, $k_p = 0.005$	Eqs. (3a), (3b)	29, 30	Data not actually fully developed
19	Compressible circular jet	x/D = 2.8	Prandtl ϵ, $k_p = 0.005$	Eqs. (3)	31	
20	Coaxial air-air jets	x/D = 0.23	As for case 19	Eqs. (3)	32, 33	
21	Coaxial H_2-air jets	x/D = 2.6	Constant eddy viscosity	Eqs. (3)	34, 35	Eddy viscosity from extrapolated τ_{mu} of ref. 10
22	Coaxial compressible H_2-air jets	x/D = 0	Maise & McDonald eddy viscosity	Eqs. (3)	36	
23	Coaxial air-air jets	---	---	---	---	Not attempted
24	Compressible plane wake	x = 1.67 cm	Laminar viscosity + constant (low) turbulent intensity	$a_2 = 1.4$	37	Computed through transition to turbulent flow

[a]Maise and McDonald eddy viscosity profiles used for boundary-layer portion of initial profile with constant ϵ (equal to one-half the adjacent Maise and McDonald value) for remainder.

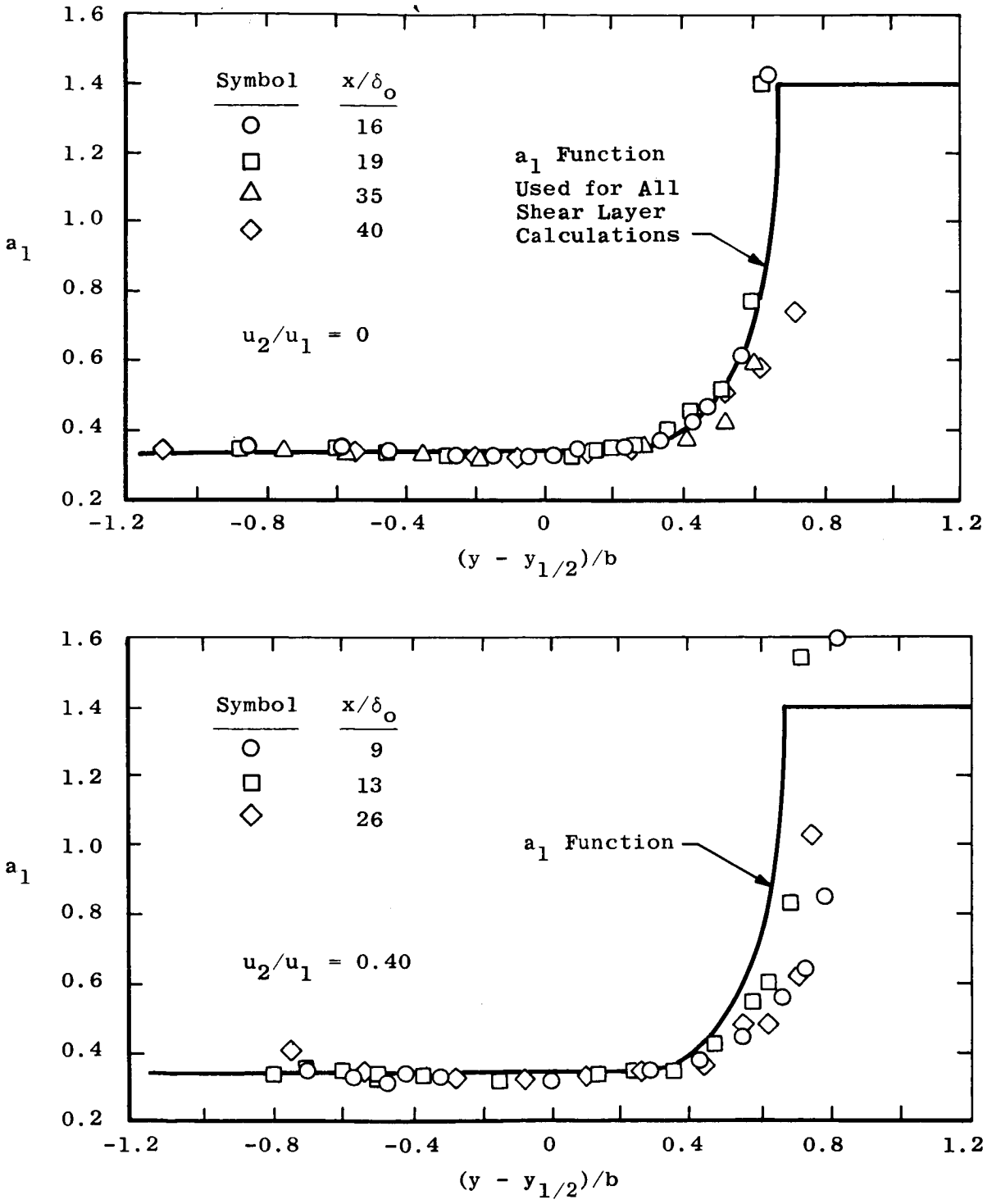

Figure 1.- Theoretical variation of parameter a_1 implied by Prandtl eddy viscosity model for two-dimensional shear layer.

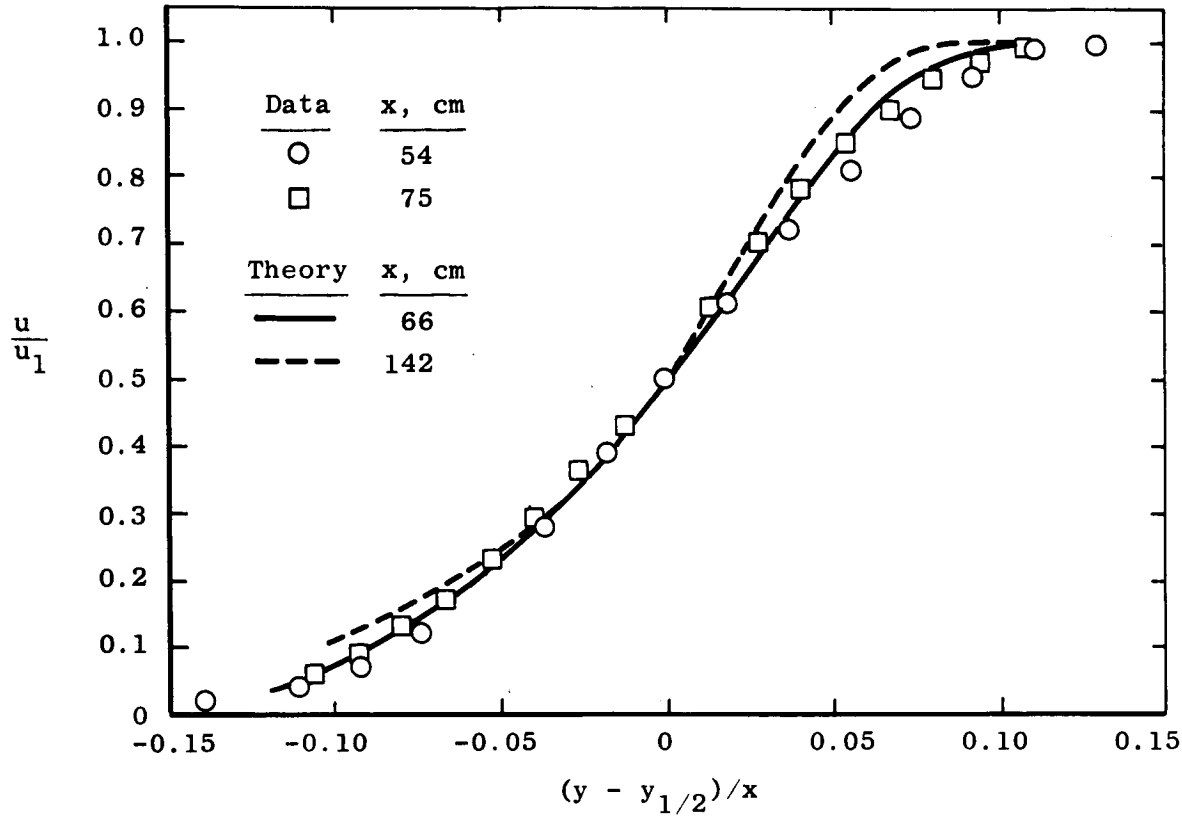

Figure 2.- Comparison of predicted shear layer velocity profile with data of Liepmann and Laufer (ref. 7) for test case 1.

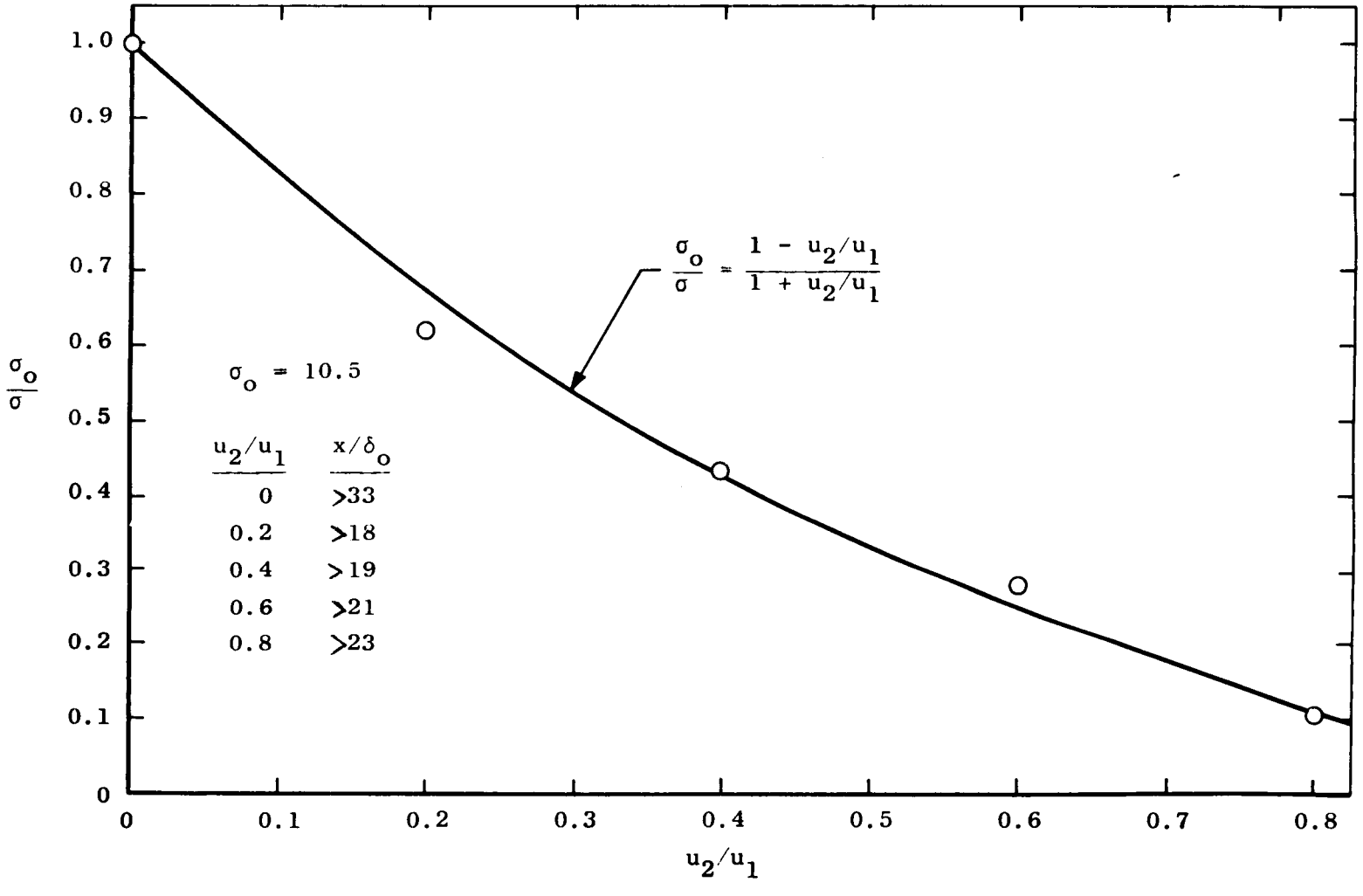

Figure 3.- Calculated variation of spreading parameter with velocity ratio for test case 1, two-dimensional shear layers.

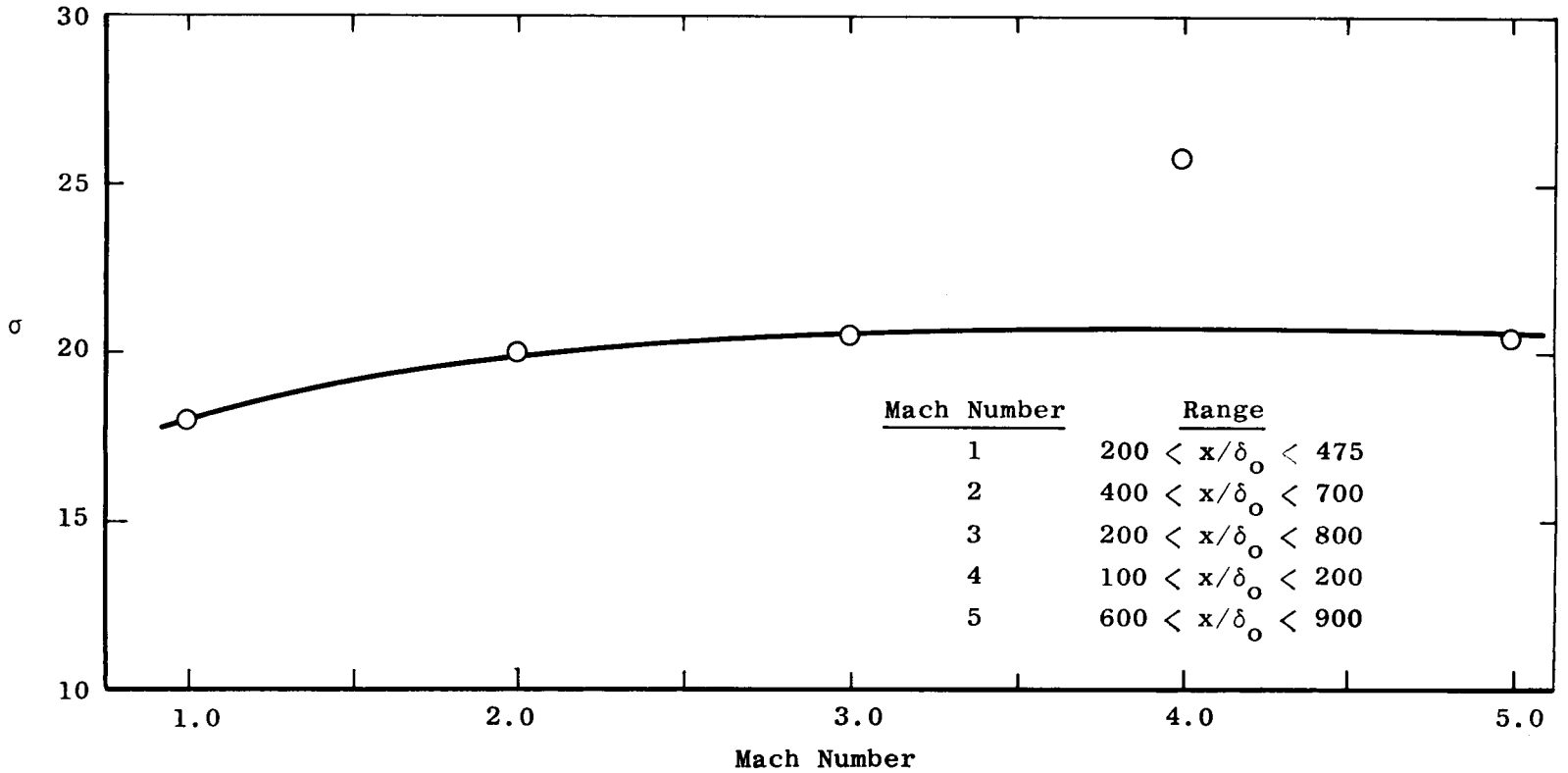

Figure 4.- Predicted variation in spreading parameter with Mach number.

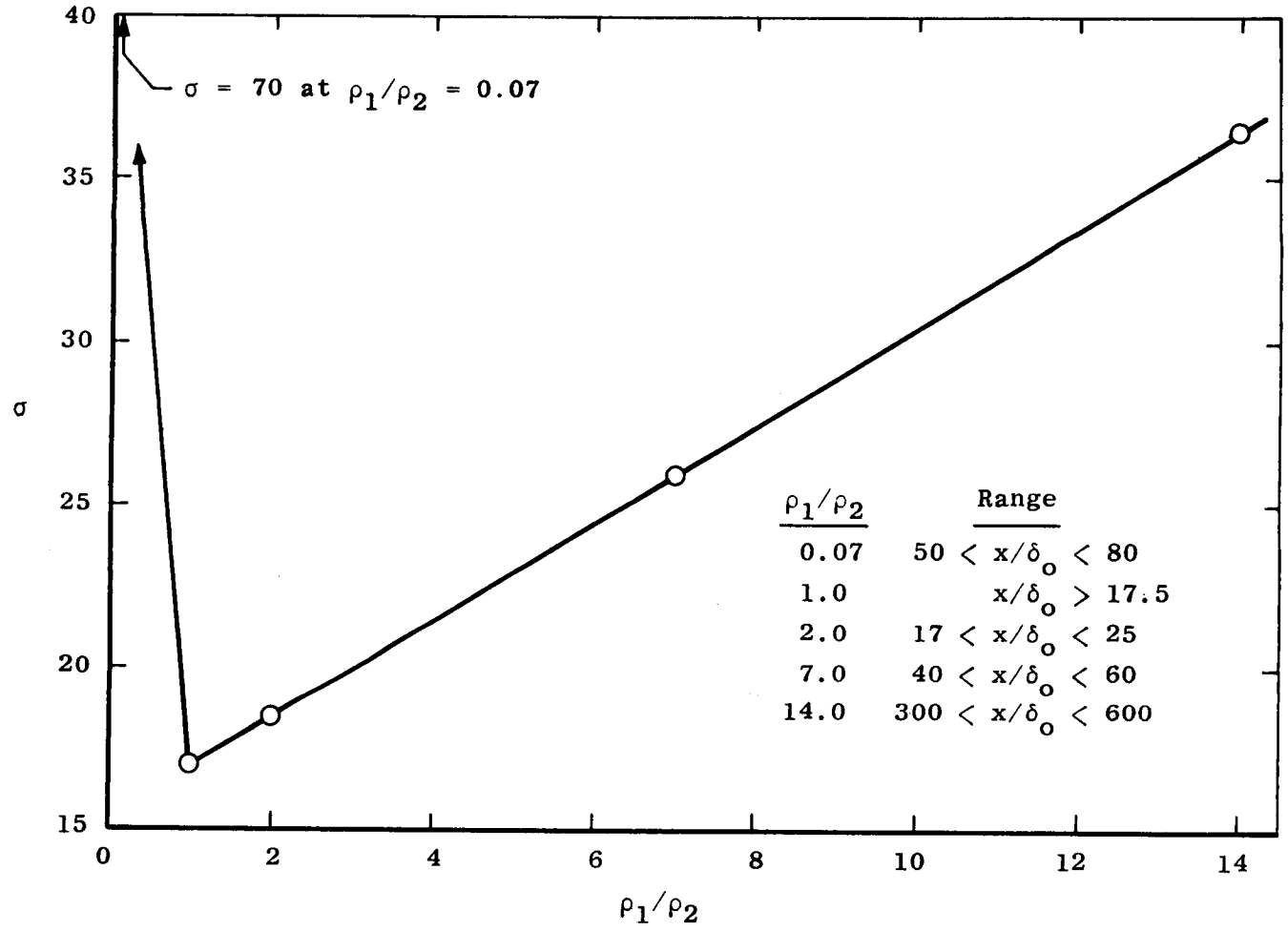

Figure 5.- Predicted variation of spreading parameter with density ratio for test case 3, two-dimensional shear layer with $u_2/u_1 = 0.2$.

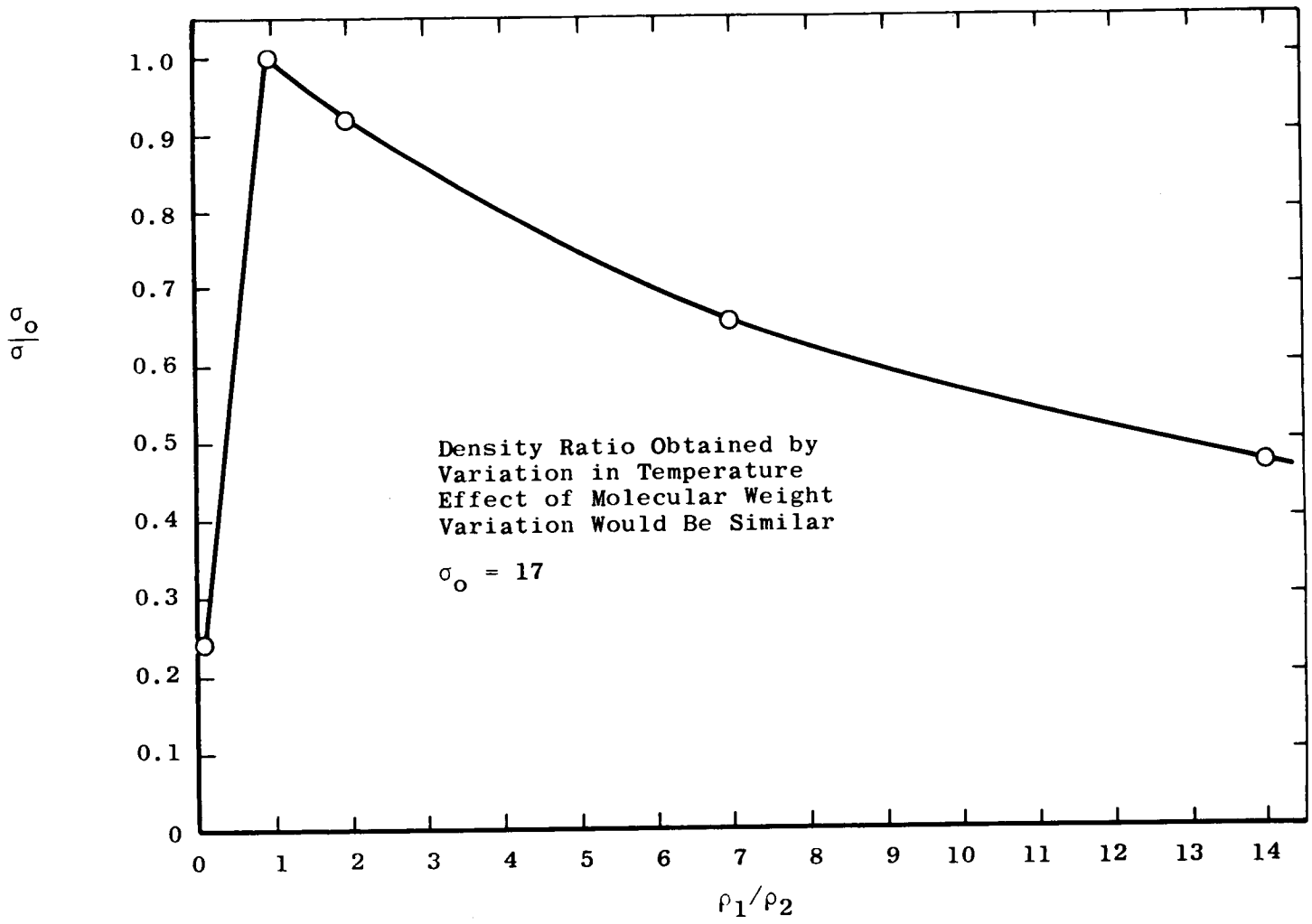

Figure 6.- Predicted variation of ratio of spread parameter to its constant-density value with density ratio for test case 3, two-dimensional shear layer with $u_2/u_1 = 0.2$.

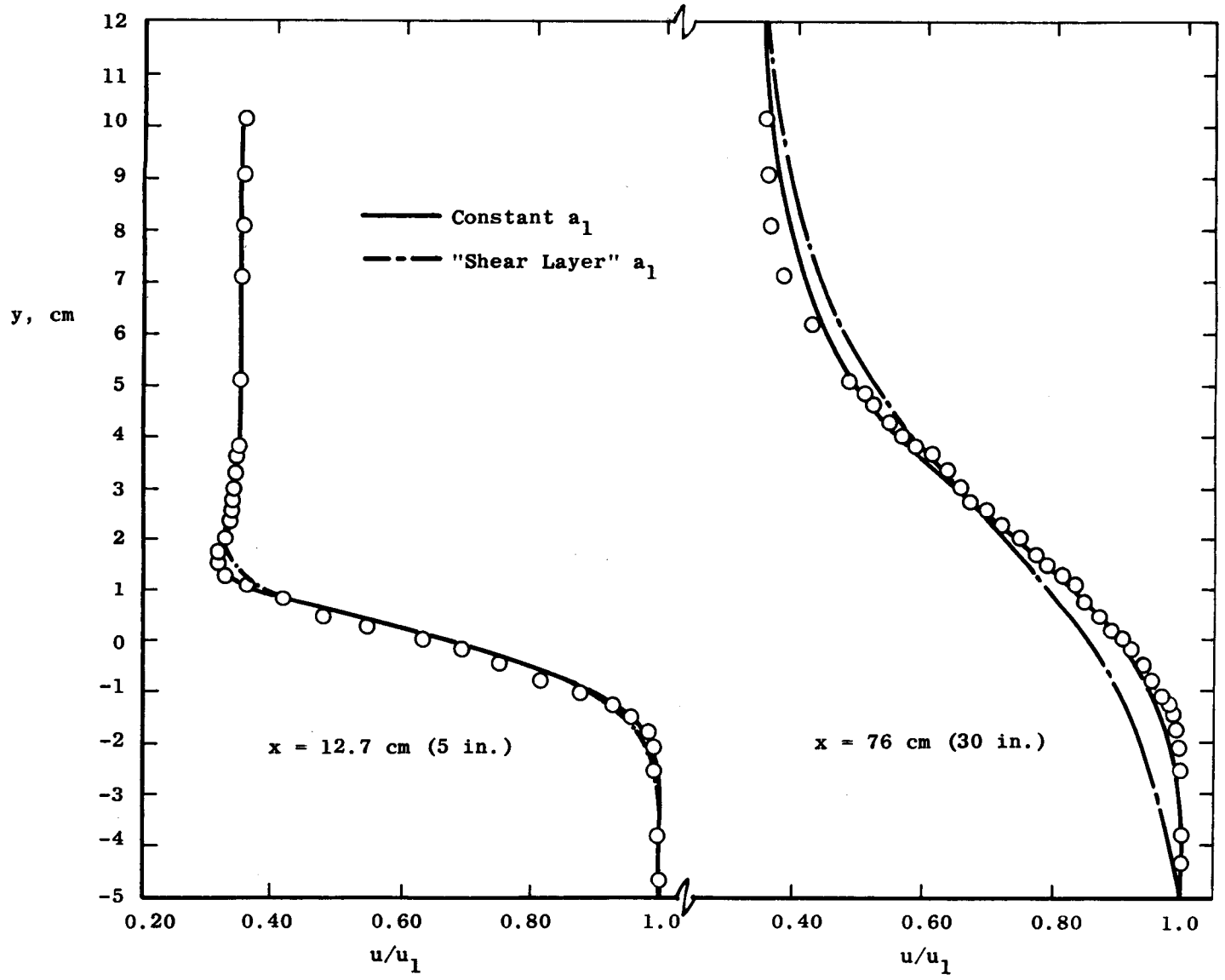

Figure 7.- Comparison of experimental and theoretical velocity profiles for test case 4, incompressible two-dimensional two-stream mixing with $u_2/u_1 = 0.357$.

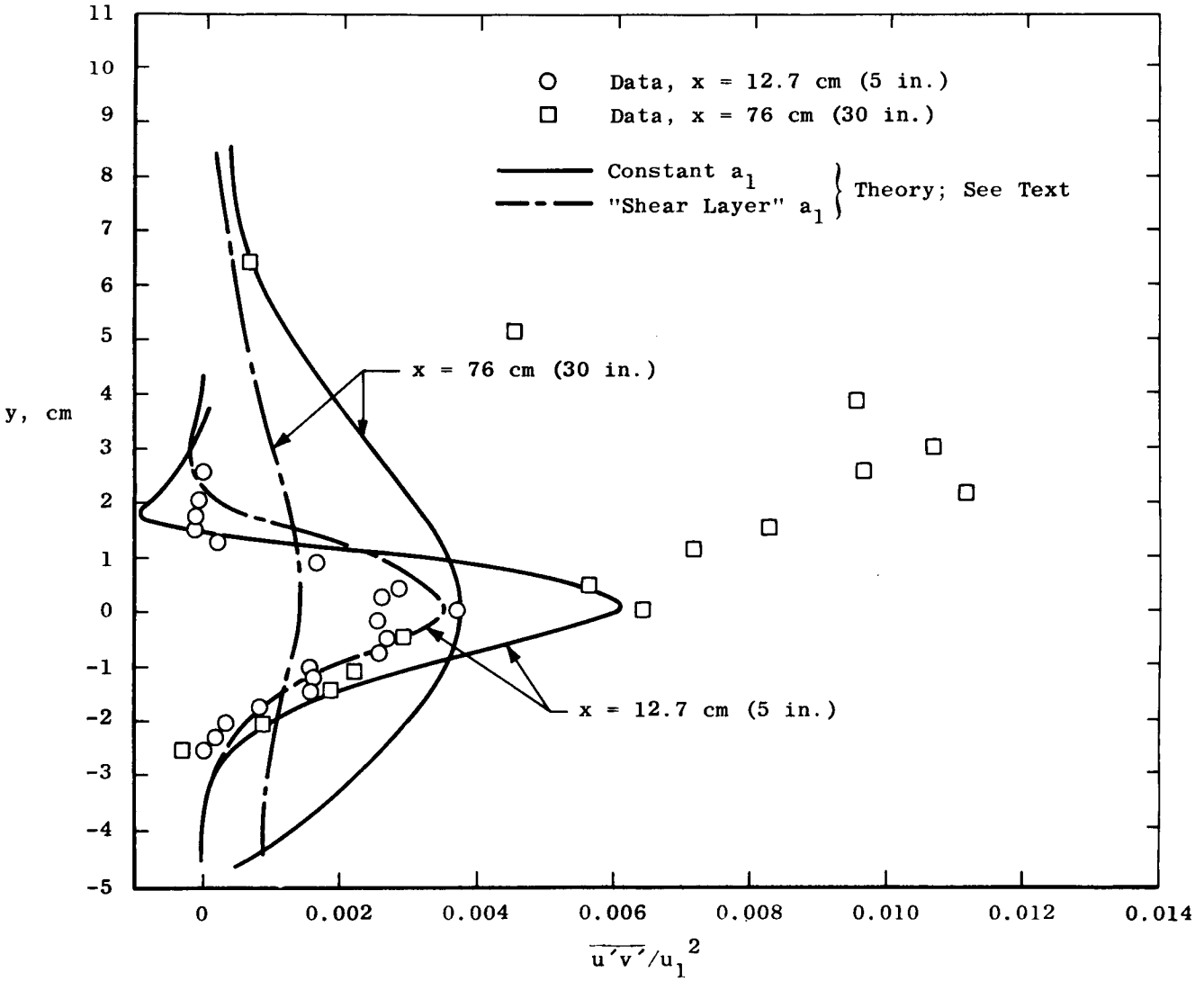

Figure 8.- Comparison of theoretical predictions of turbulent shear stress with experimental data for test case 4.

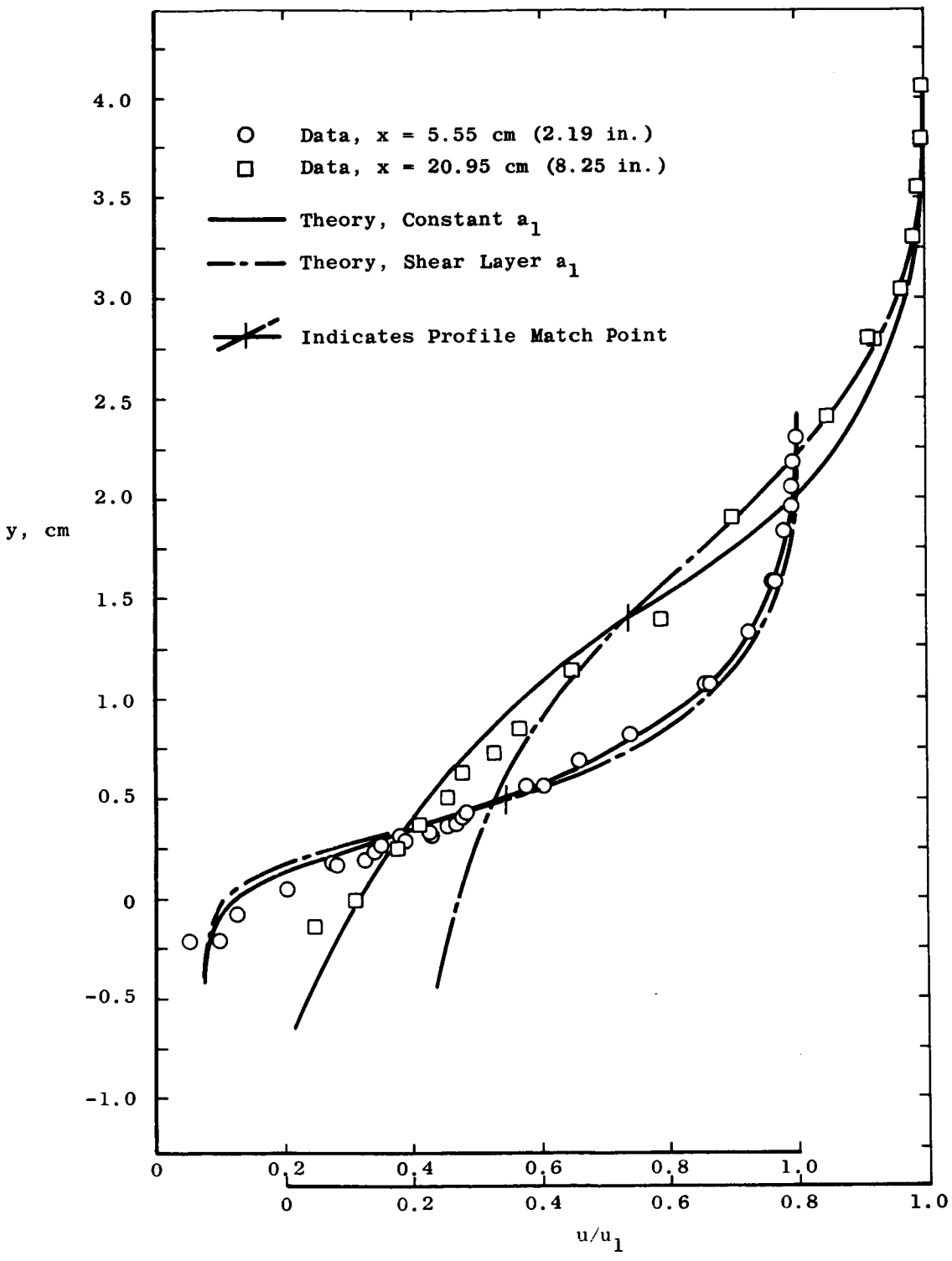

Figure 9.- Comparison of theoretical and experimental profiles for test case 5, compressible two-dimensional shear layer.

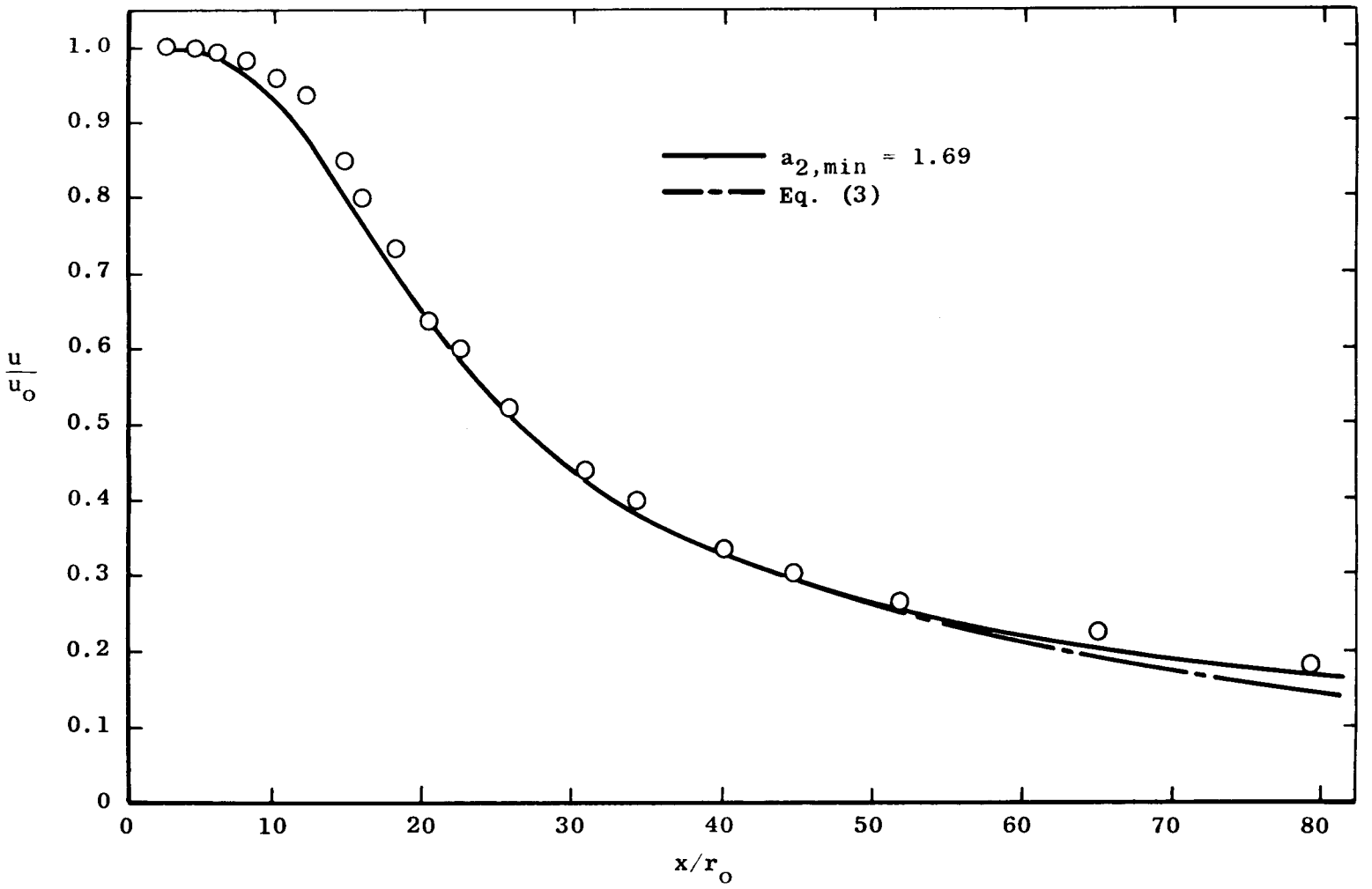

Figure 10.- Comparison of theoretical and experimental center-line velocity decay for test case 6, circular jet.

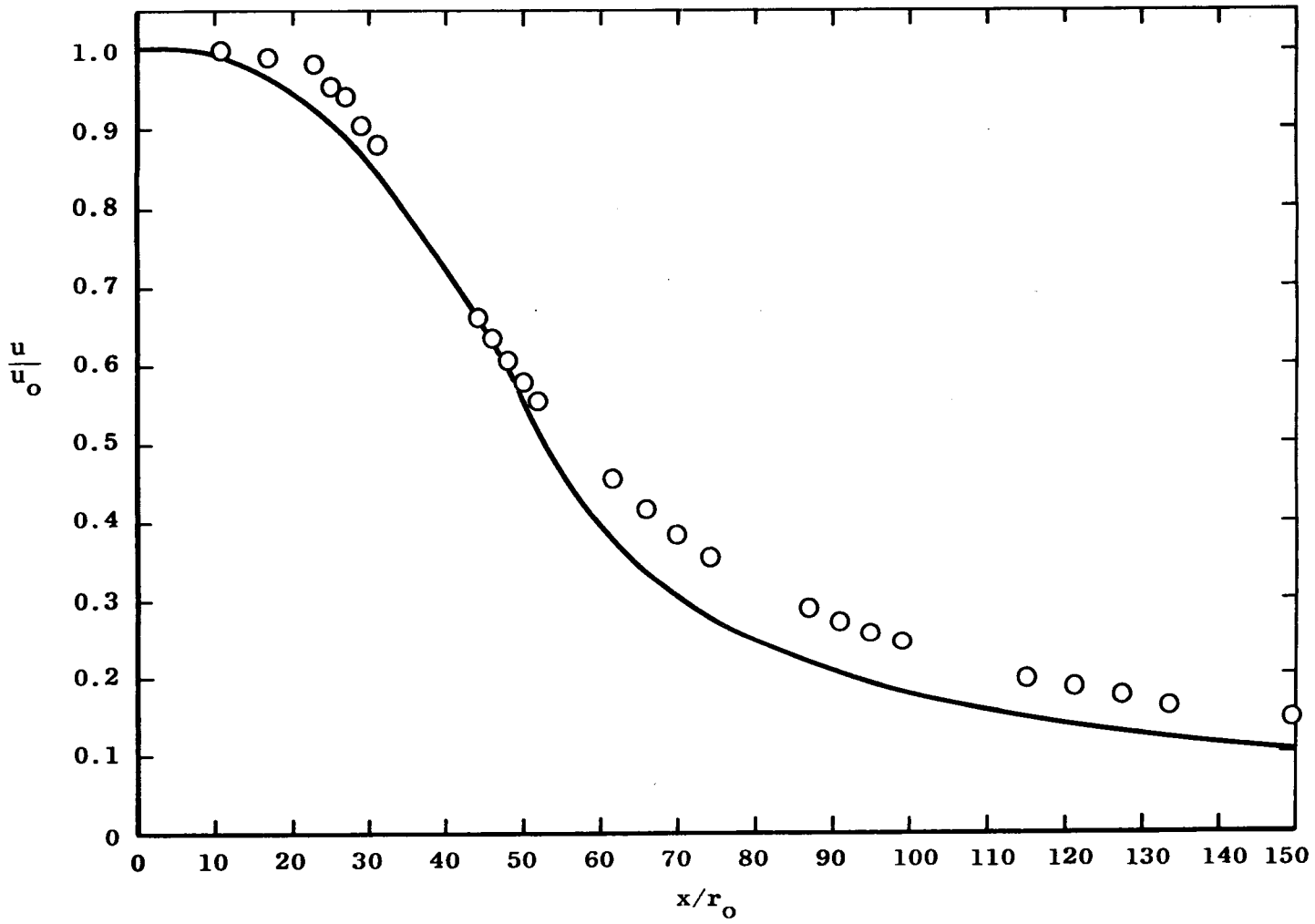

Figure 11.- Comparison of experimental and theoretical center-line velocity decay for test case 7, $M_o = 2.22$ circular jet.

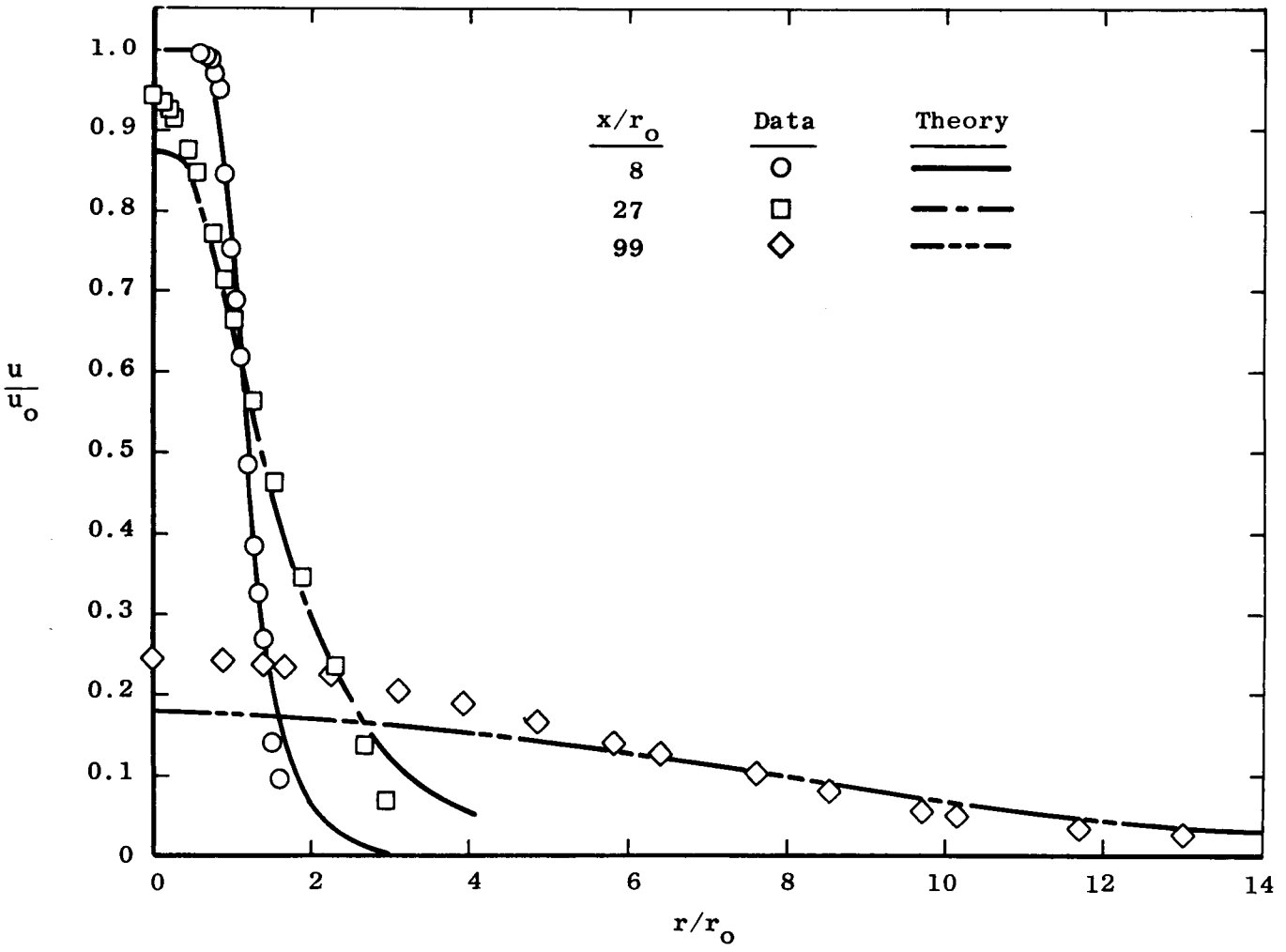

Figure 12.- Comparison of theoretical and experimental velocity profiles for test case 7, $M_o = 2.22$ circular jet. Data from reference 8.

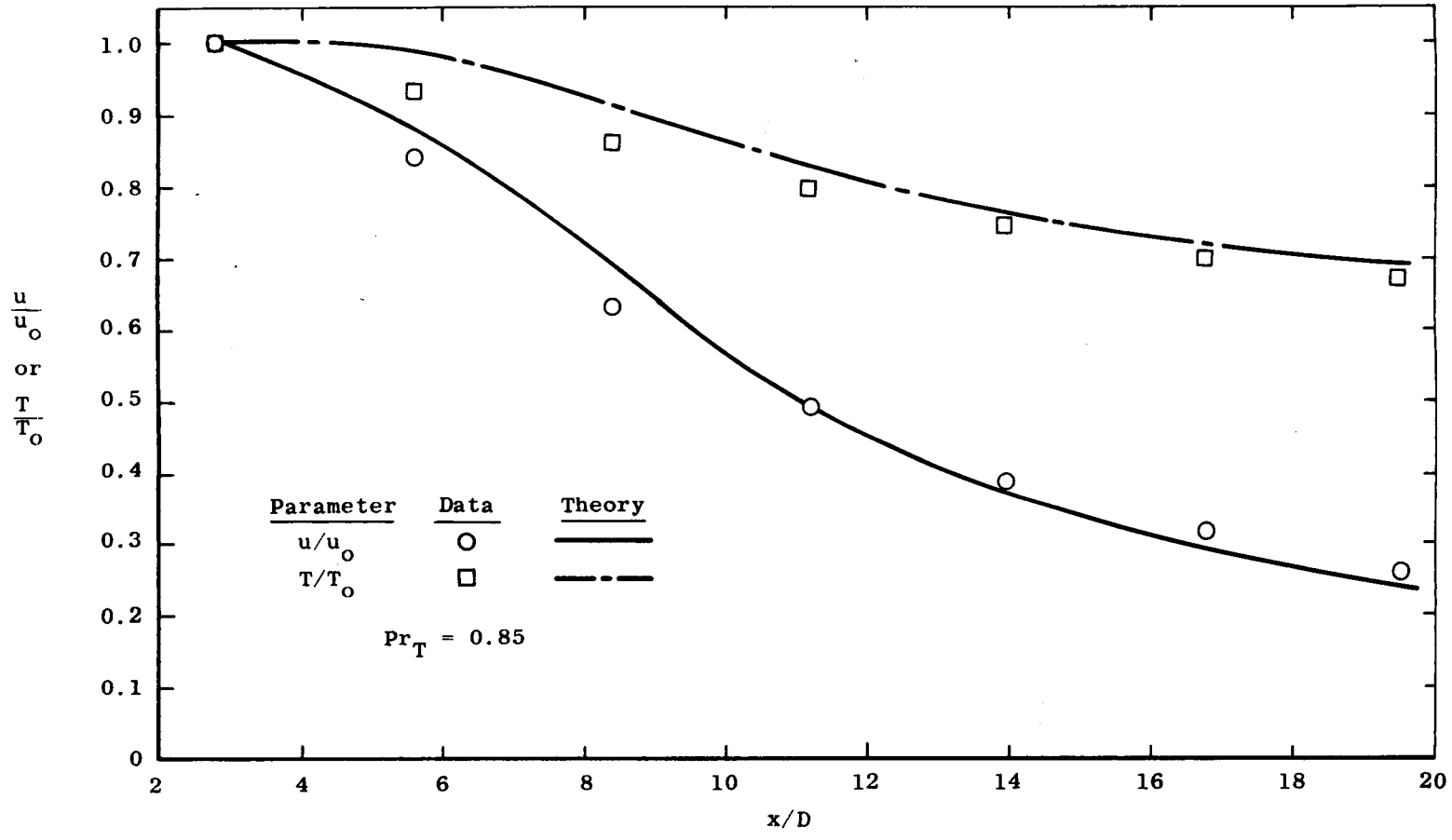

Figure 13.- Comparison of experimental and theoretical decay of center-line velocity and static temperature for test case 8, $M_o = 0.7$ circular jet.

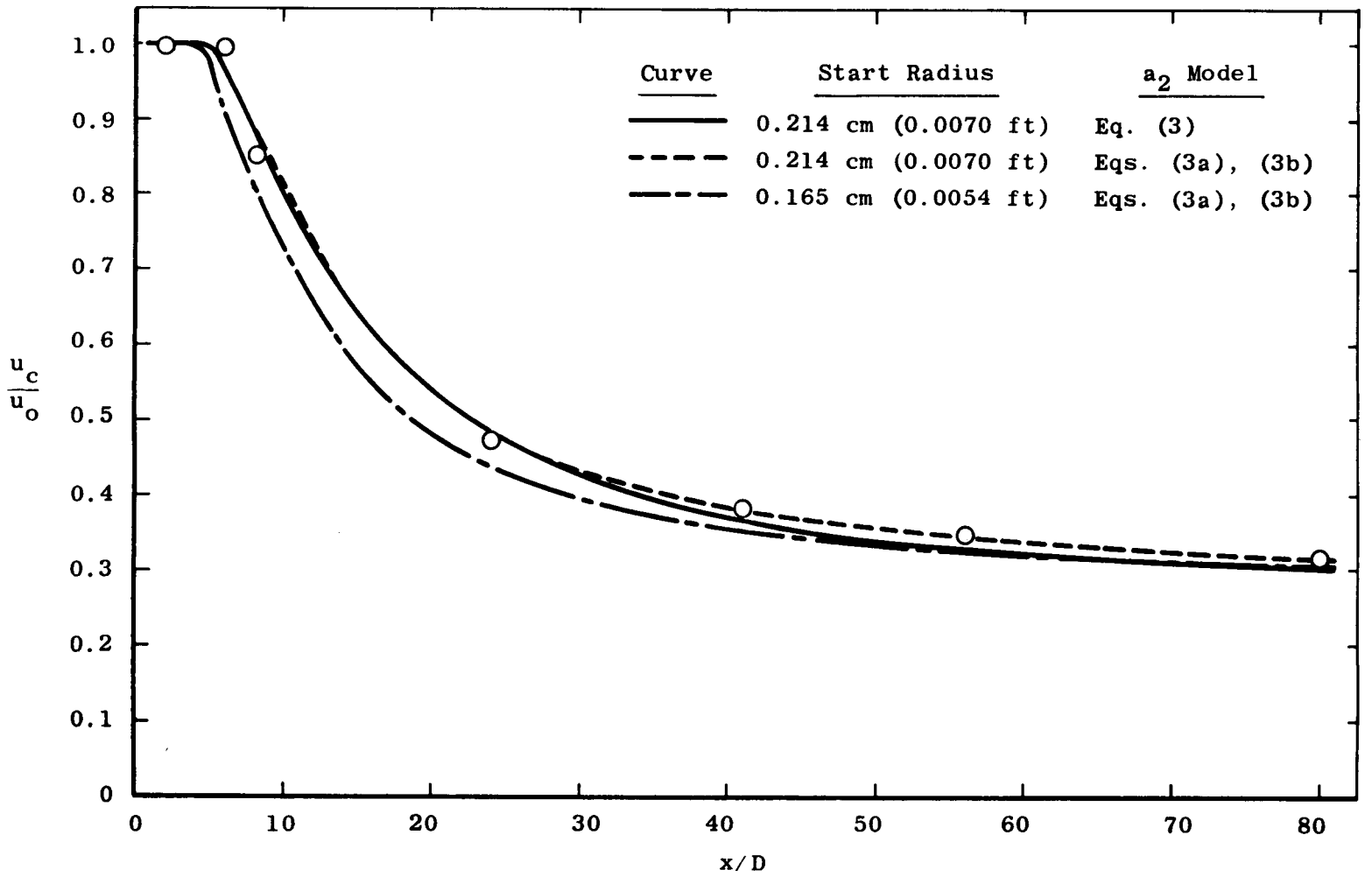

Figure 14.- Comparison of calculated center-line velocity with experiment for test case 9, coaxial air jets with He trace.

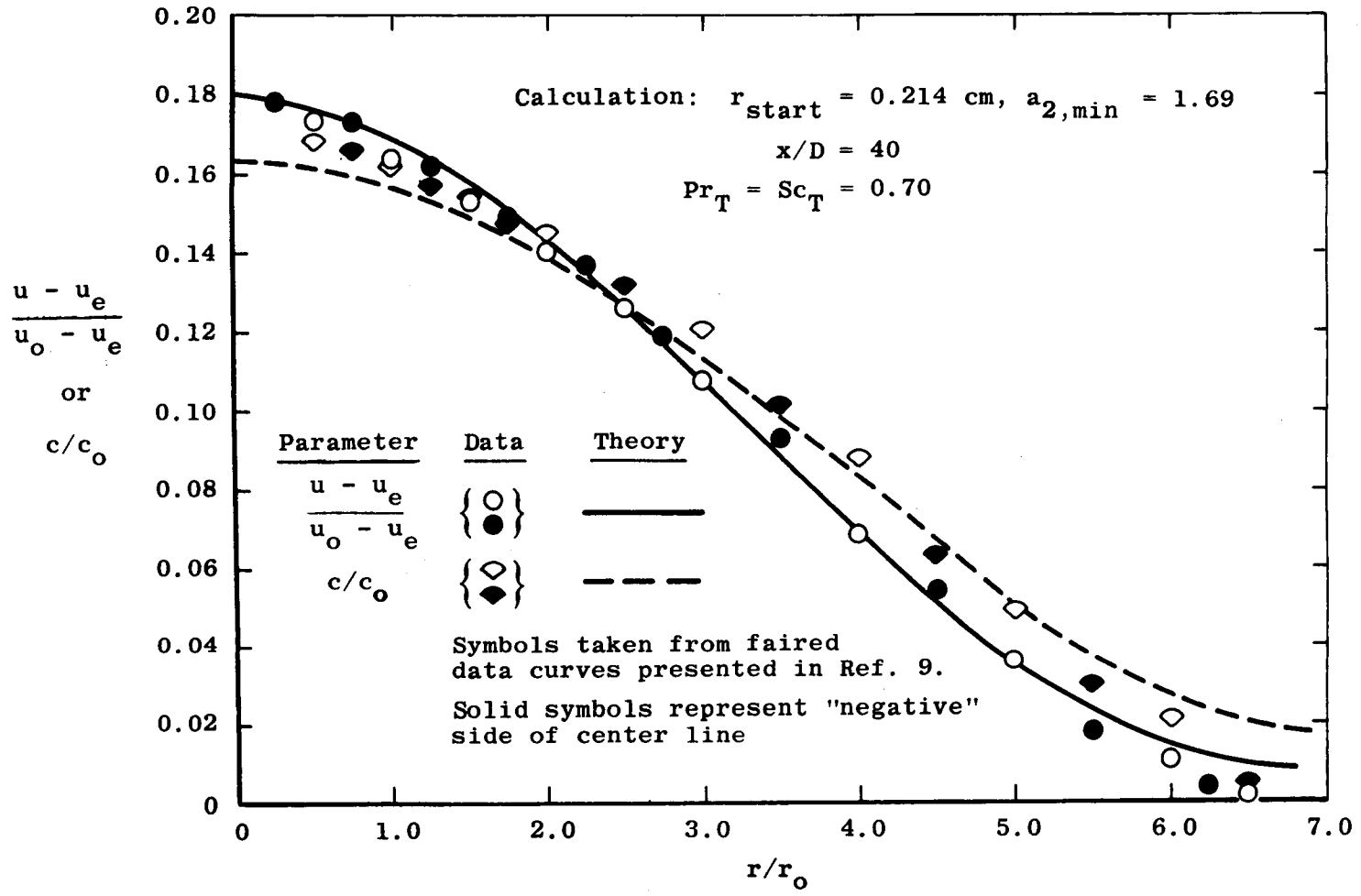

Figure 15.- Comparison of theoretical and experimental velocity and concentration profiles for test case 9.

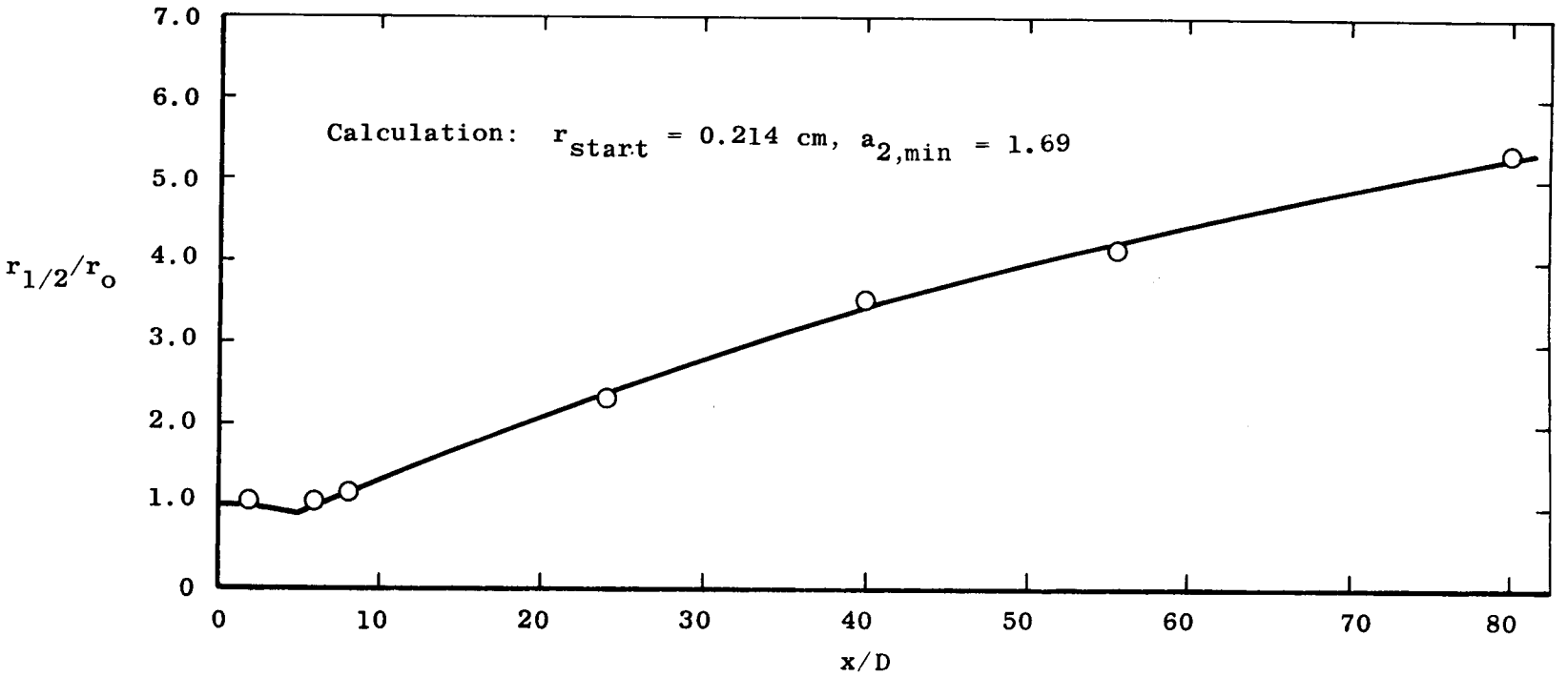

Figure 16.- Comparison of predicted and experimental half-velocity radius for test case 9.

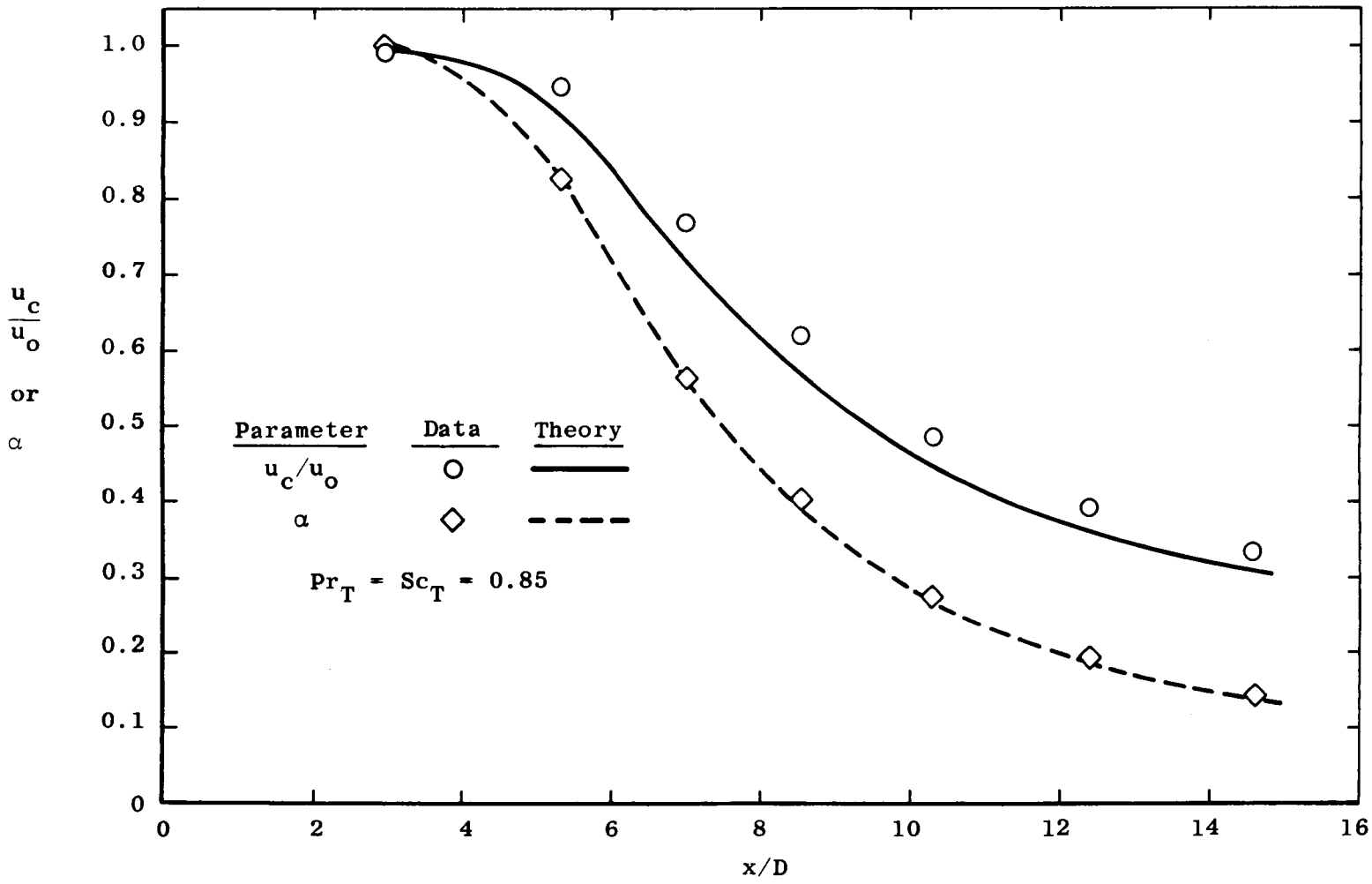

Figure 17.- Comparison of theoretical prediction of center-line decay with experimental data for test case 10, H_2-air jets.

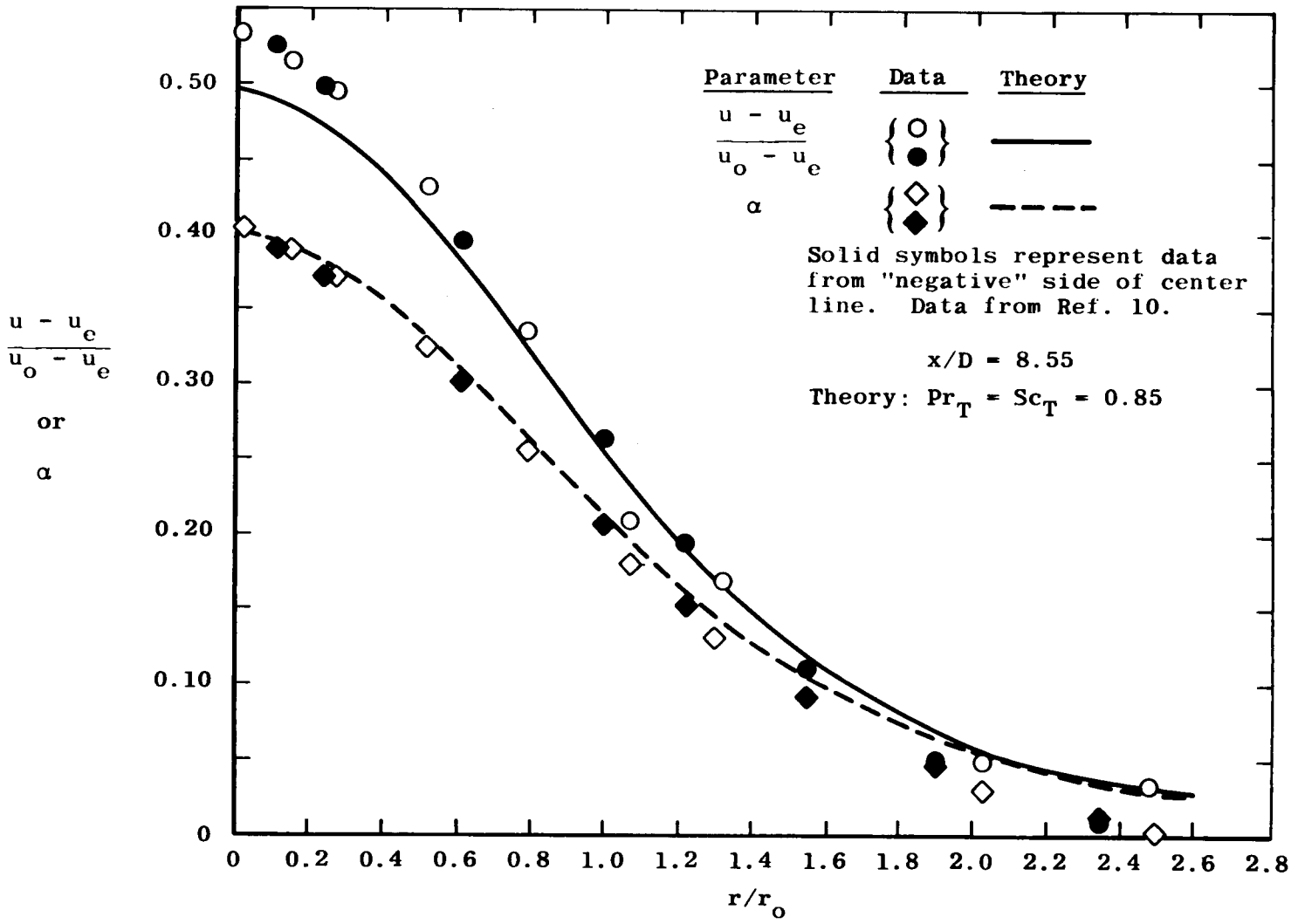

Figure 18.- Comparison of predicted and experimental radial profiles for test case 10, coaxial H_2-air.

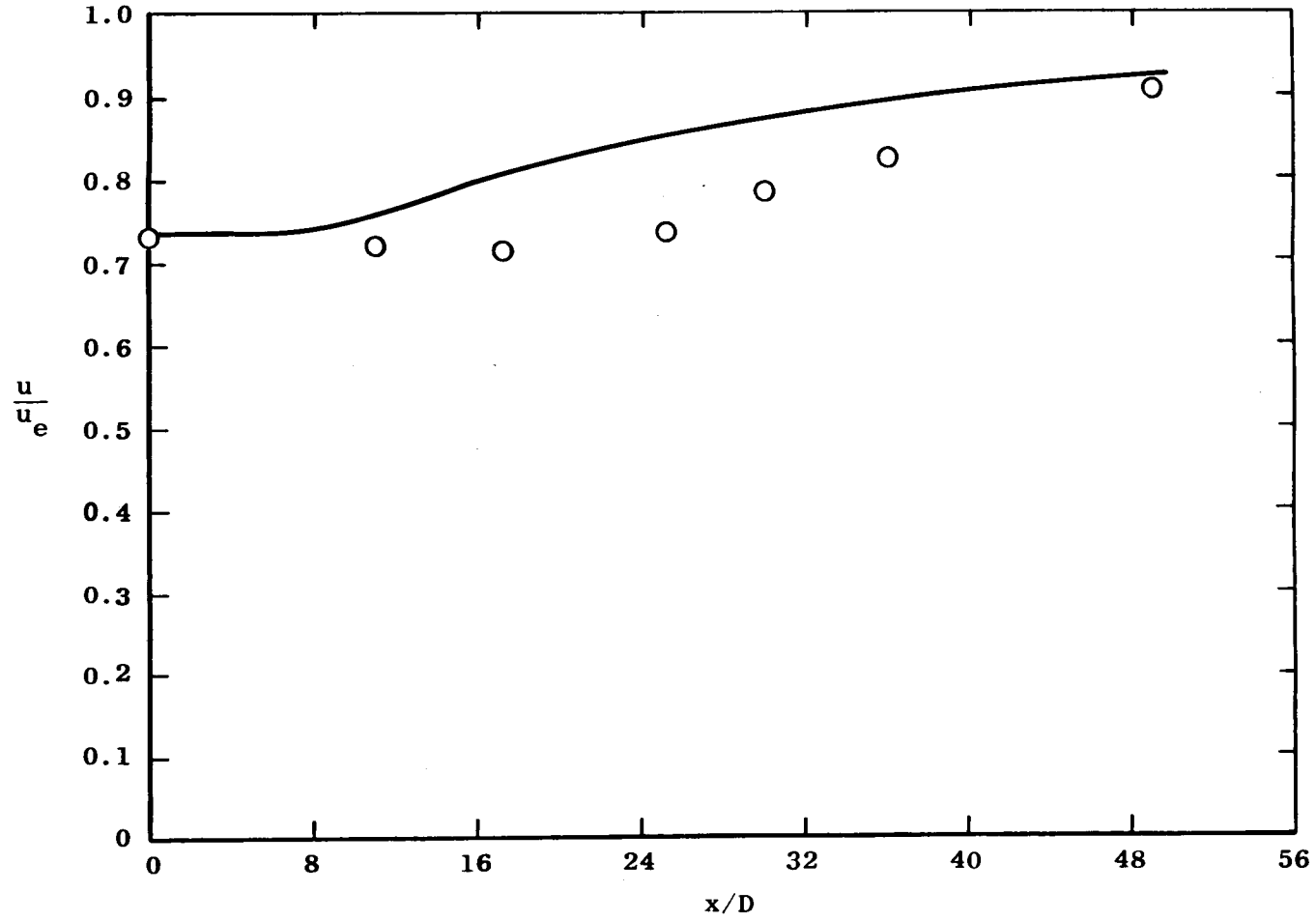

Figure 19.- Comparison of theoretical and experimental center-line velocity ratio for test case 11, axisymmetric jet in moving stream $M_o = 0.90$, $M_e = 1.30$.

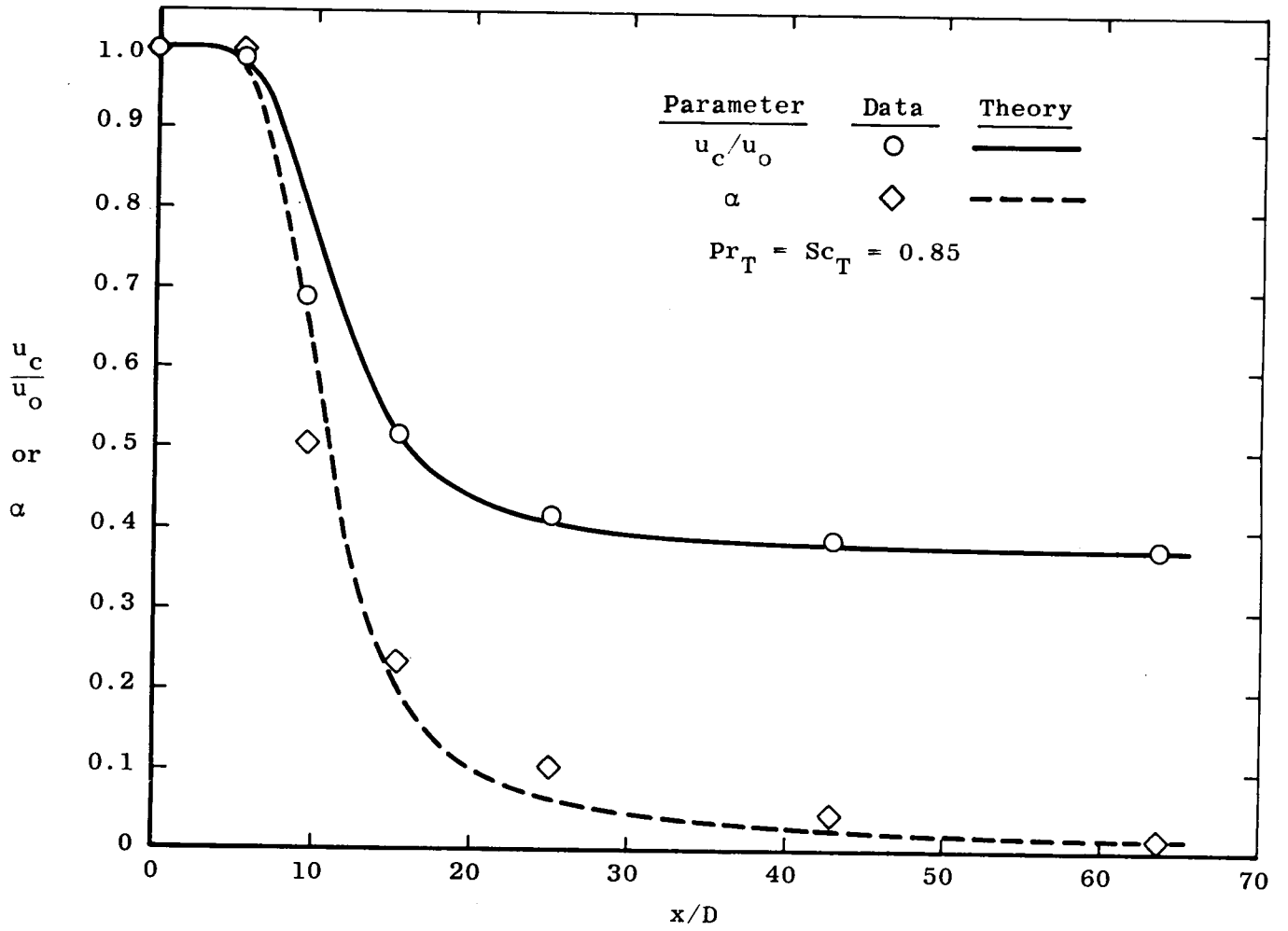

Figure 20.- Comparison of center-line velocity and jet species concentration decay predictions with experiment for test case 12, coaxial H_2-air jets.

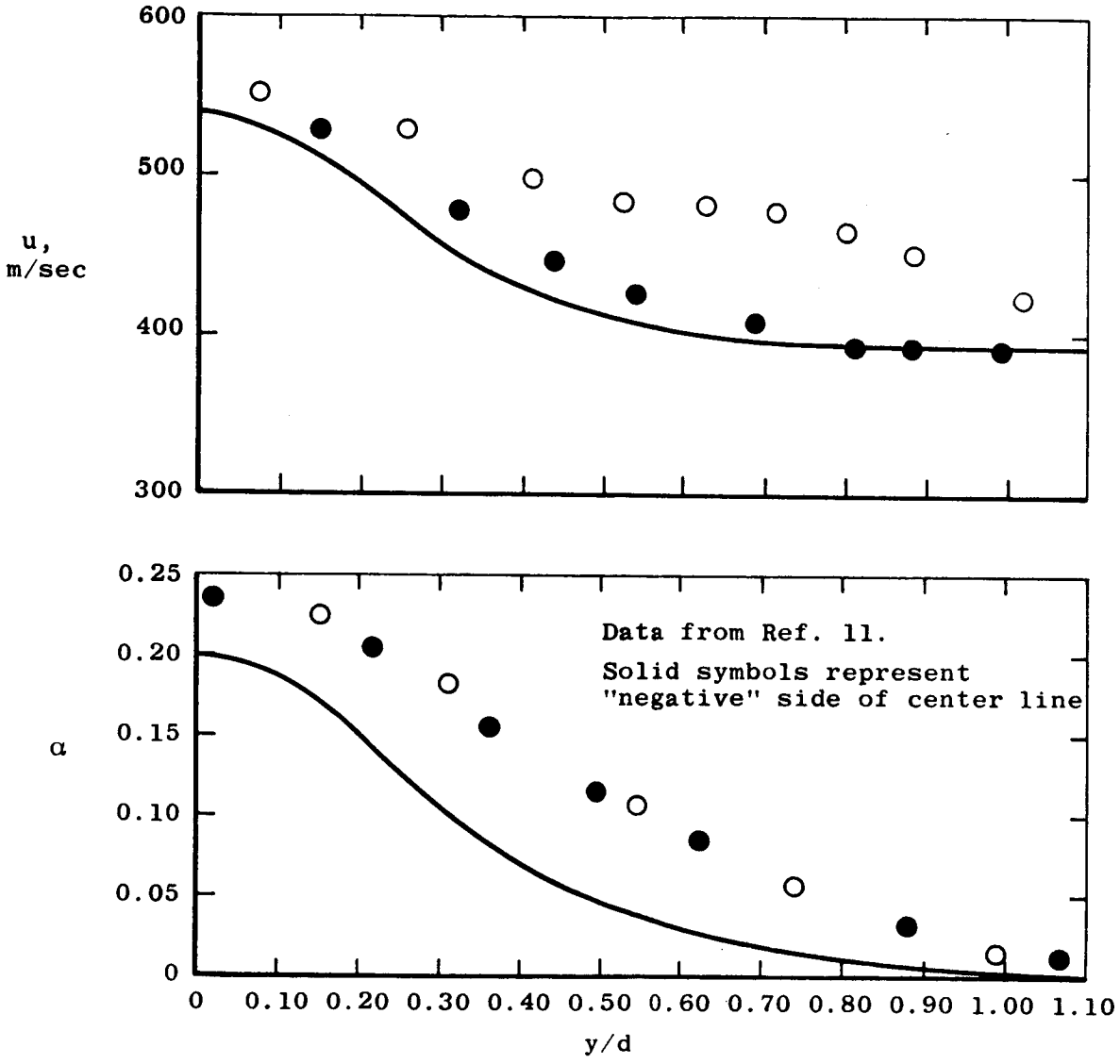

Figure 21.- Comparison of theoretical and experimental profiles for test case 12. x/D = 15.4.

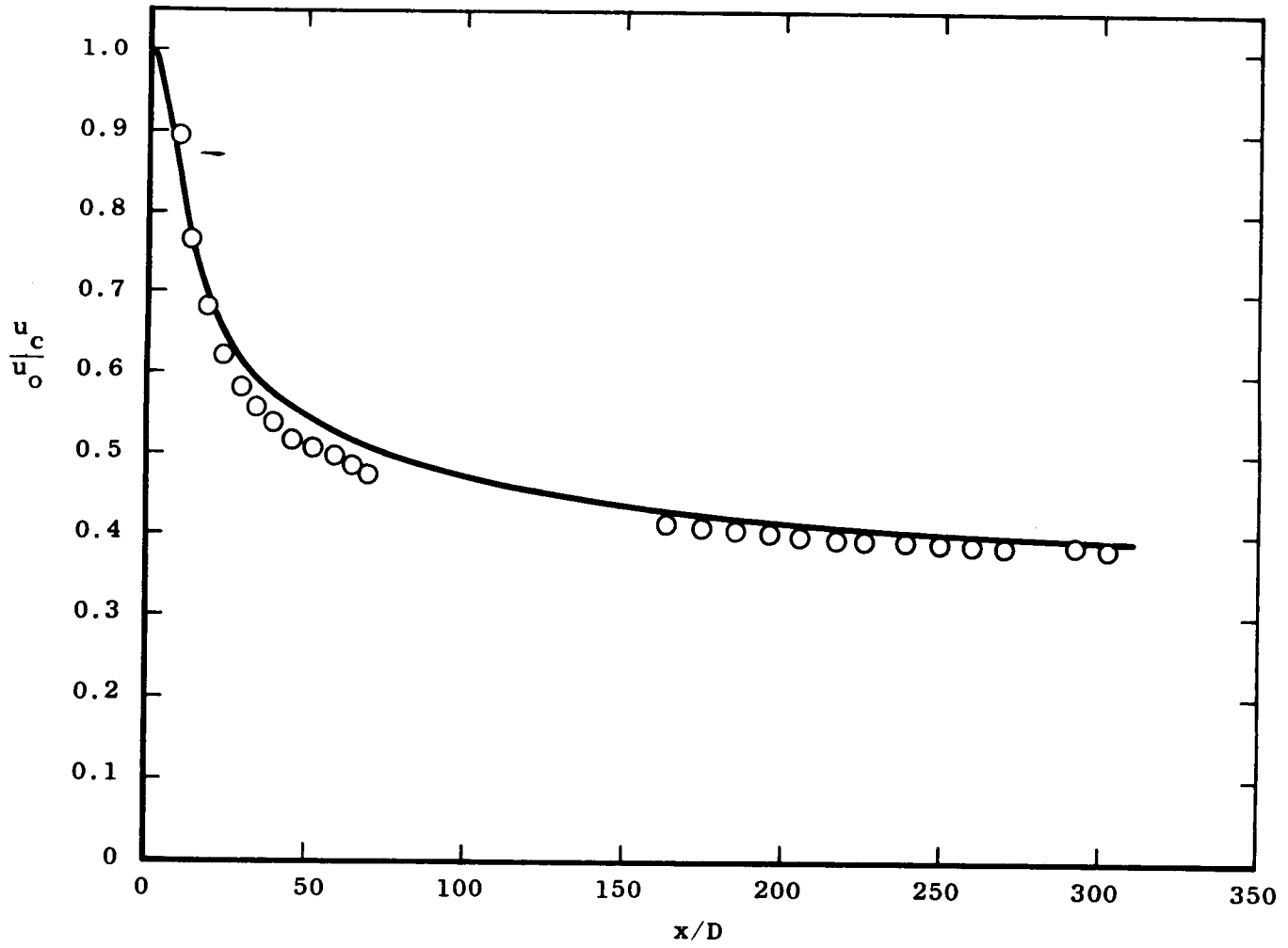

Figure 22.- Comparison of center-line velocity prediction with data for test case 13, two-dimensional jet with $u_o/u_e = 3.29$.

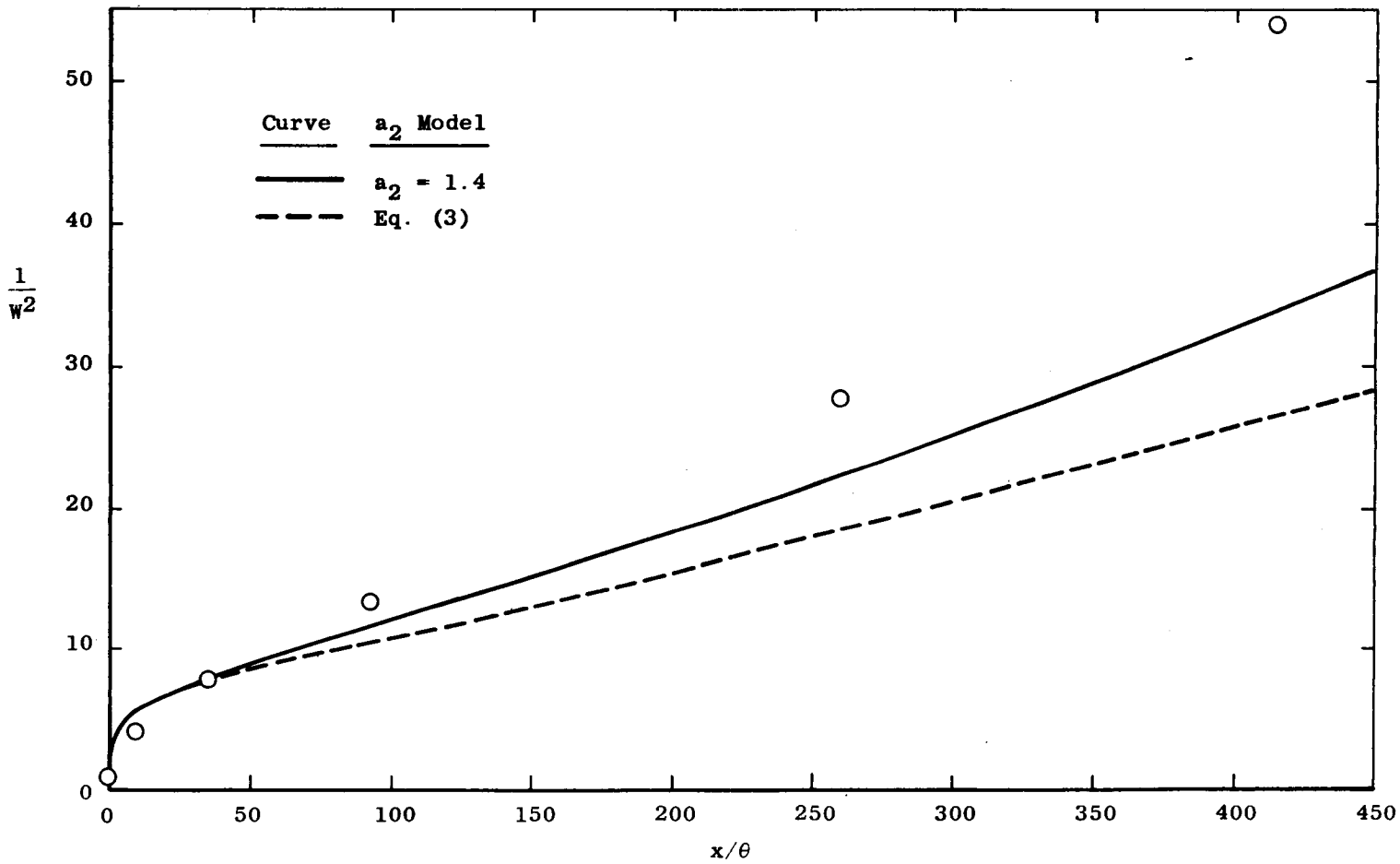

Figure 23.- Comparison of experimental center-line velocity increase with prediction for test case 14, two-dimensional wake.

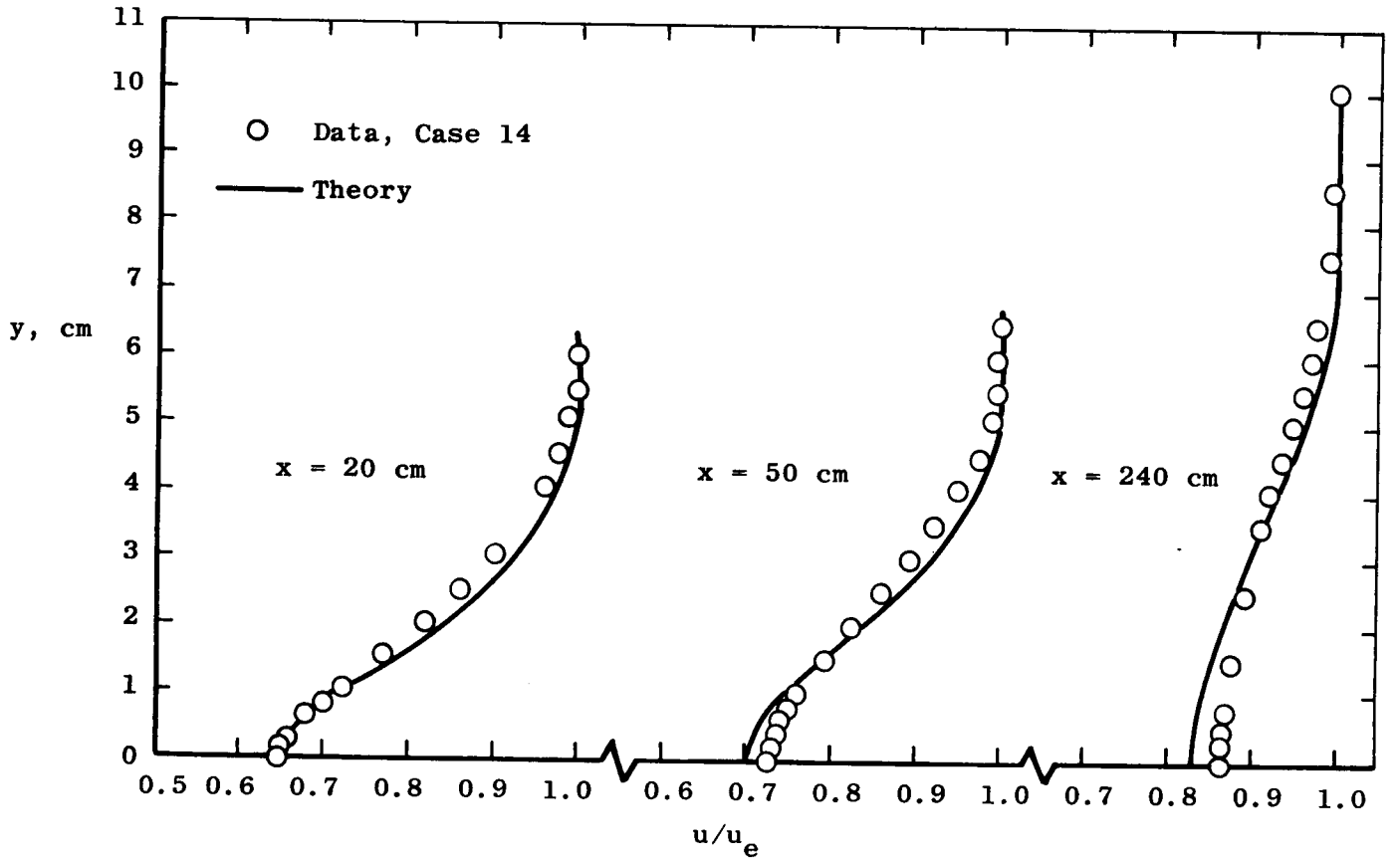

Figure 24.- Comparison of predicted velocity profiles with experimental data for test case 14, two-dimensional wake.

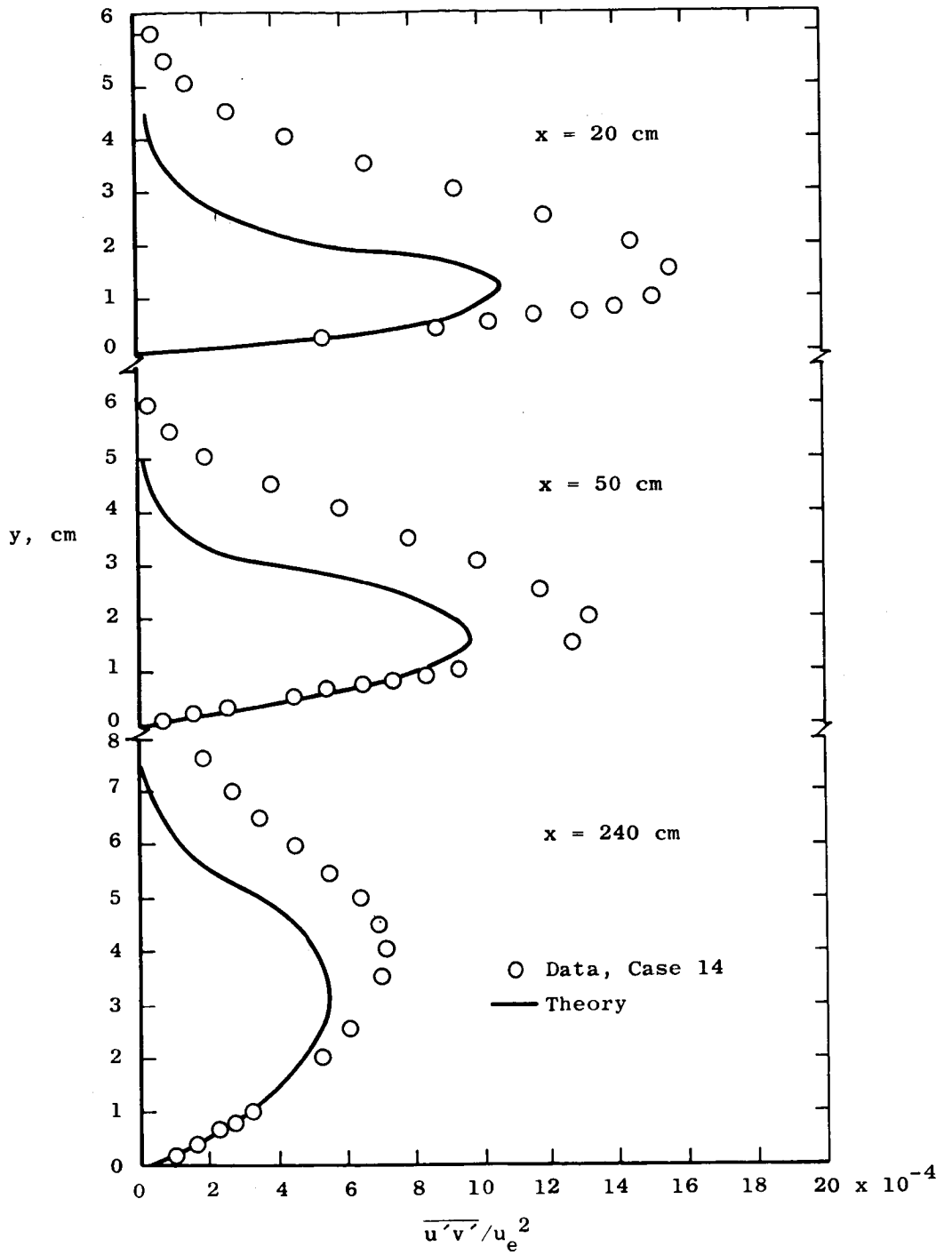

Figure 25.- Comparison of predicted turbulent shear stress with experimental data for test case 14.

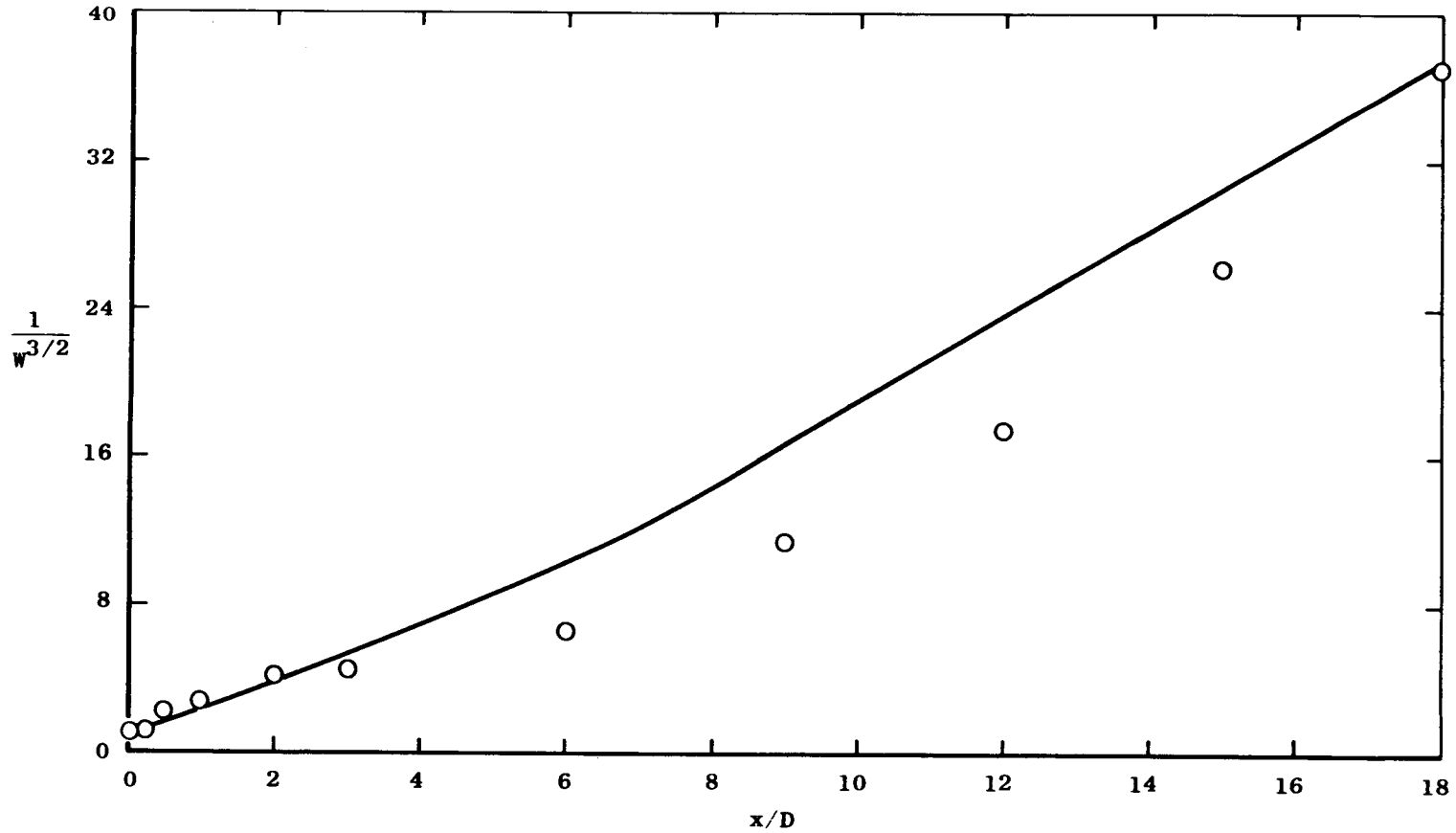

Figure 26.- Comparison of theoretical prediction of center-line velocity with experiment for test case 15, axisymmetric wake.

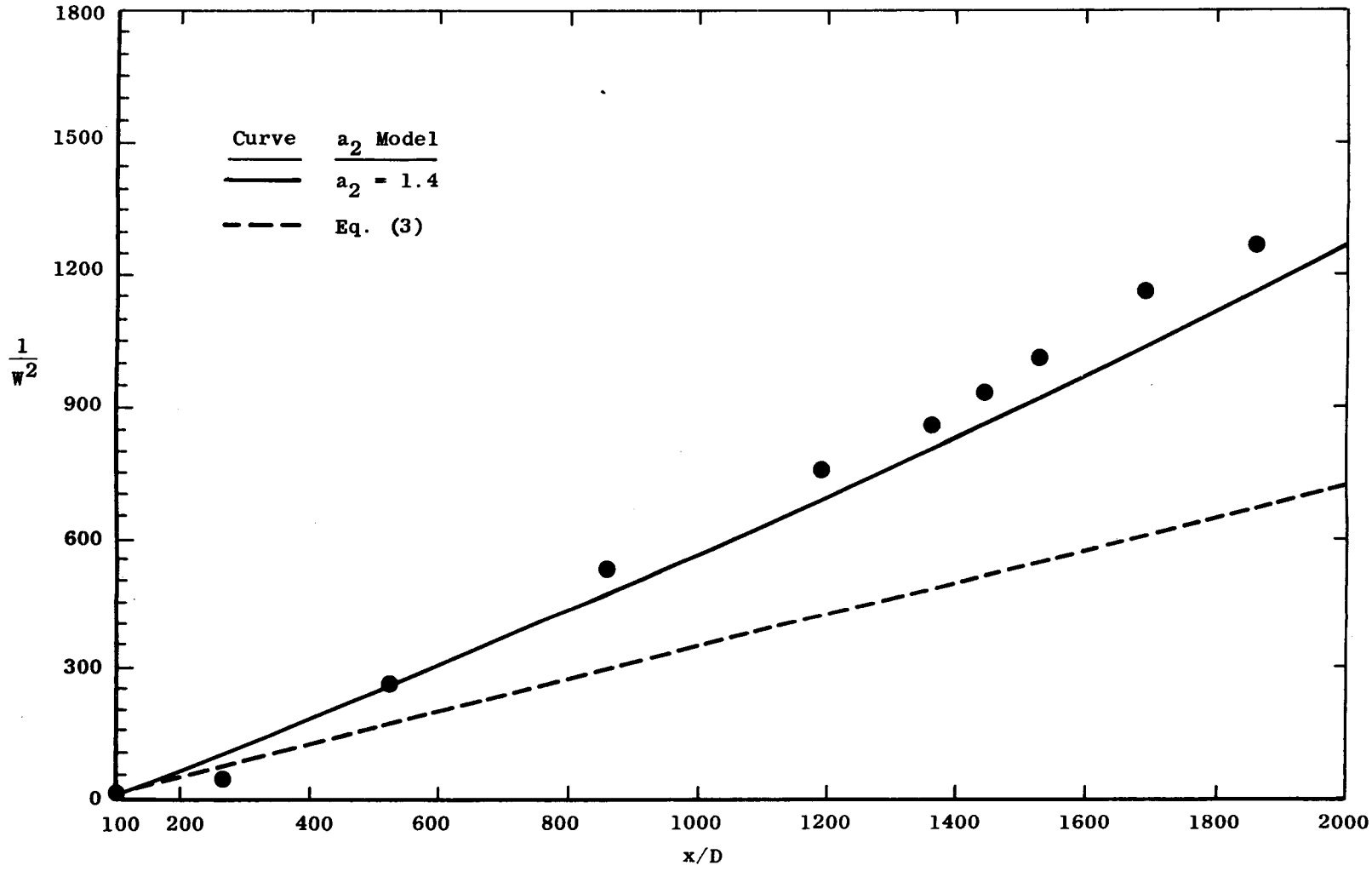

Figure 27.- Comparison of calculated and experimental center-line velocities for test case 16, compressible plane wake, D = 0.00909 cm.

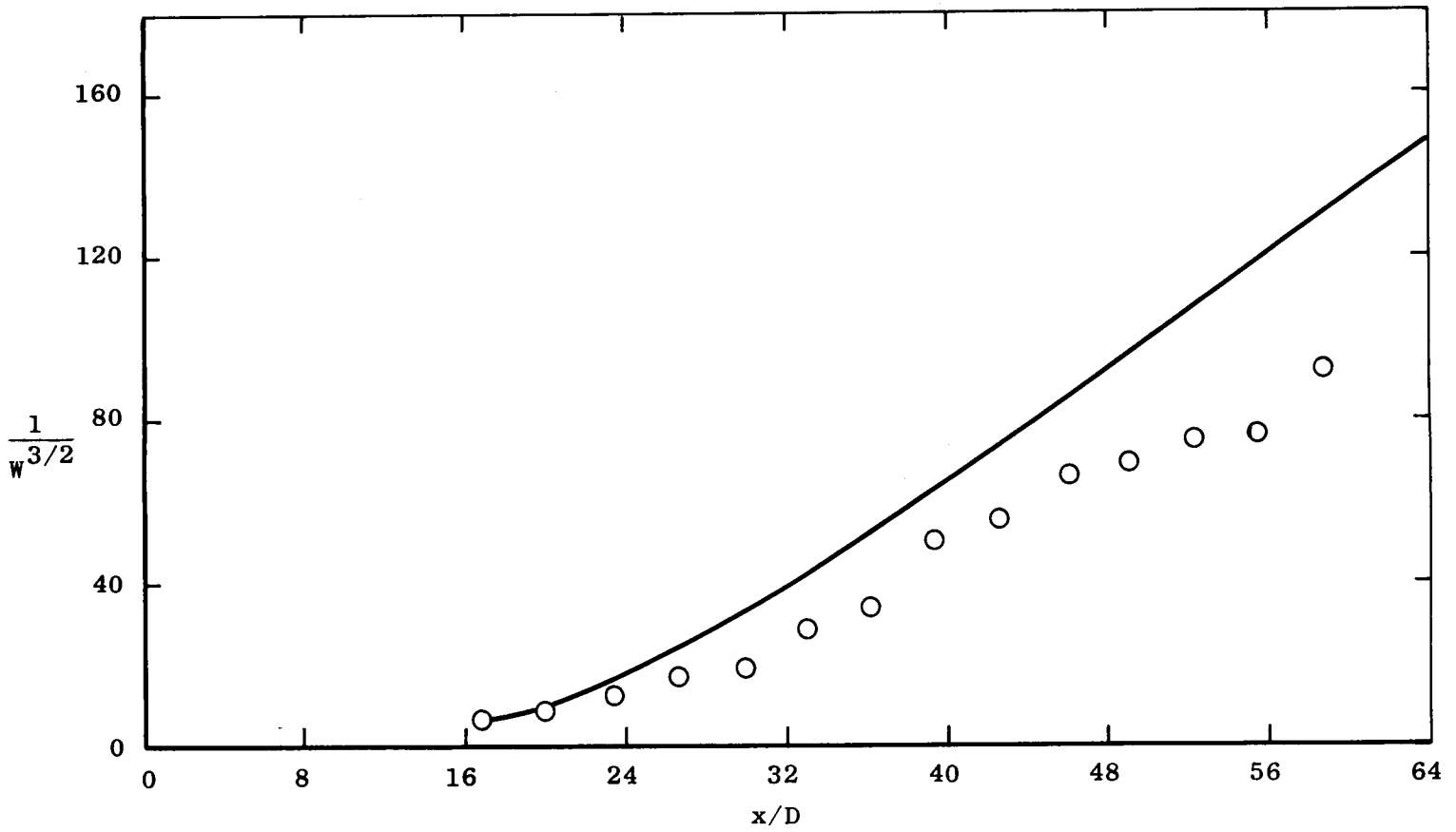

Figure 28.- Comparison of theoretical and experimental center-line velocity ratio for test case 17, compressible axisymmetric wake.

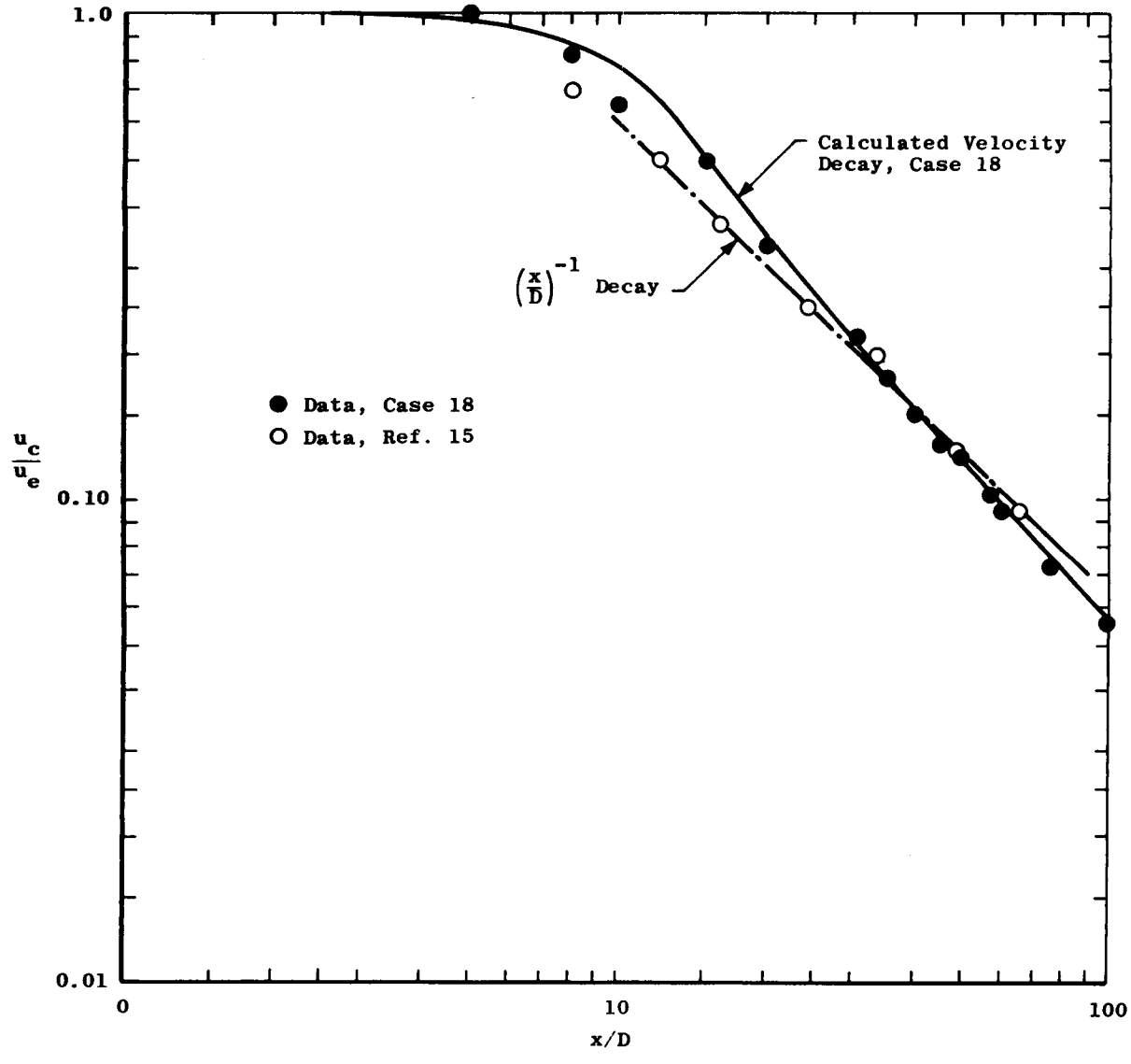

Figure 29.- Comparison of theoretical and experimental center-line velocity decay for test case 18, asymptotic jet.

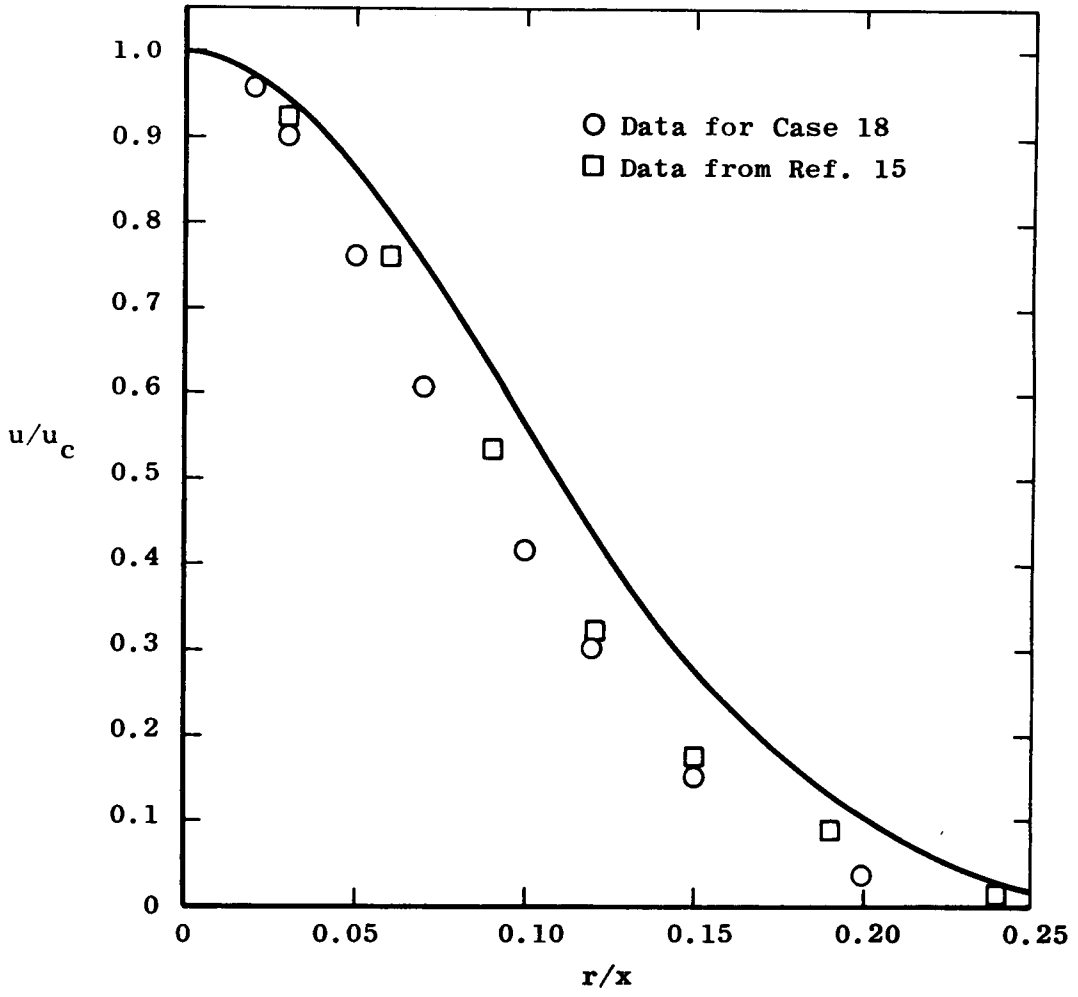

Figure 30.- Comparison of theoretical and experimental axial velocity profiles for test case 18, circular jet.

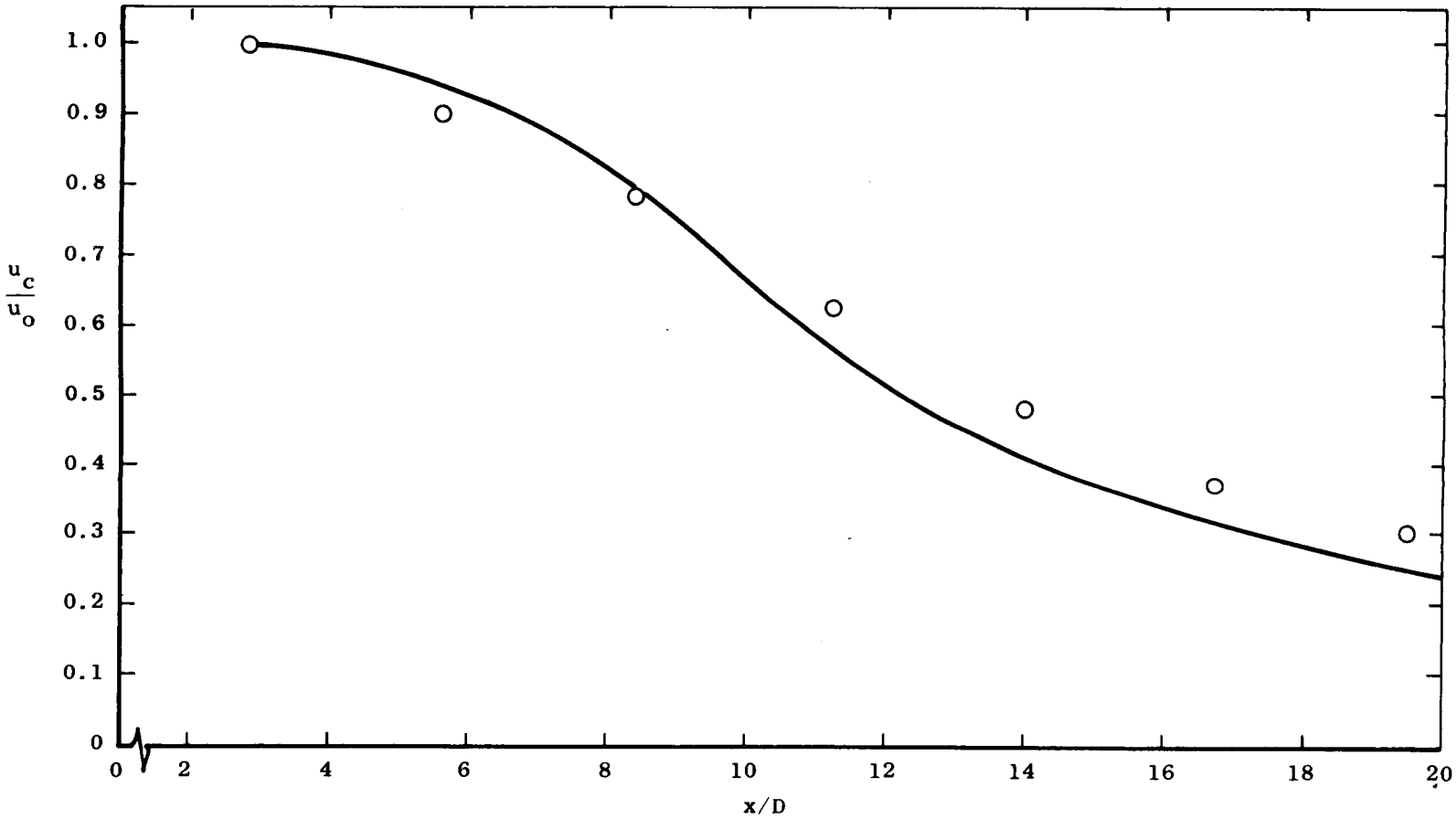

Figure 31.- Comparison of predicted center-line velocity decay with experiment for test case 19, $M_o = 1.4$ jet.

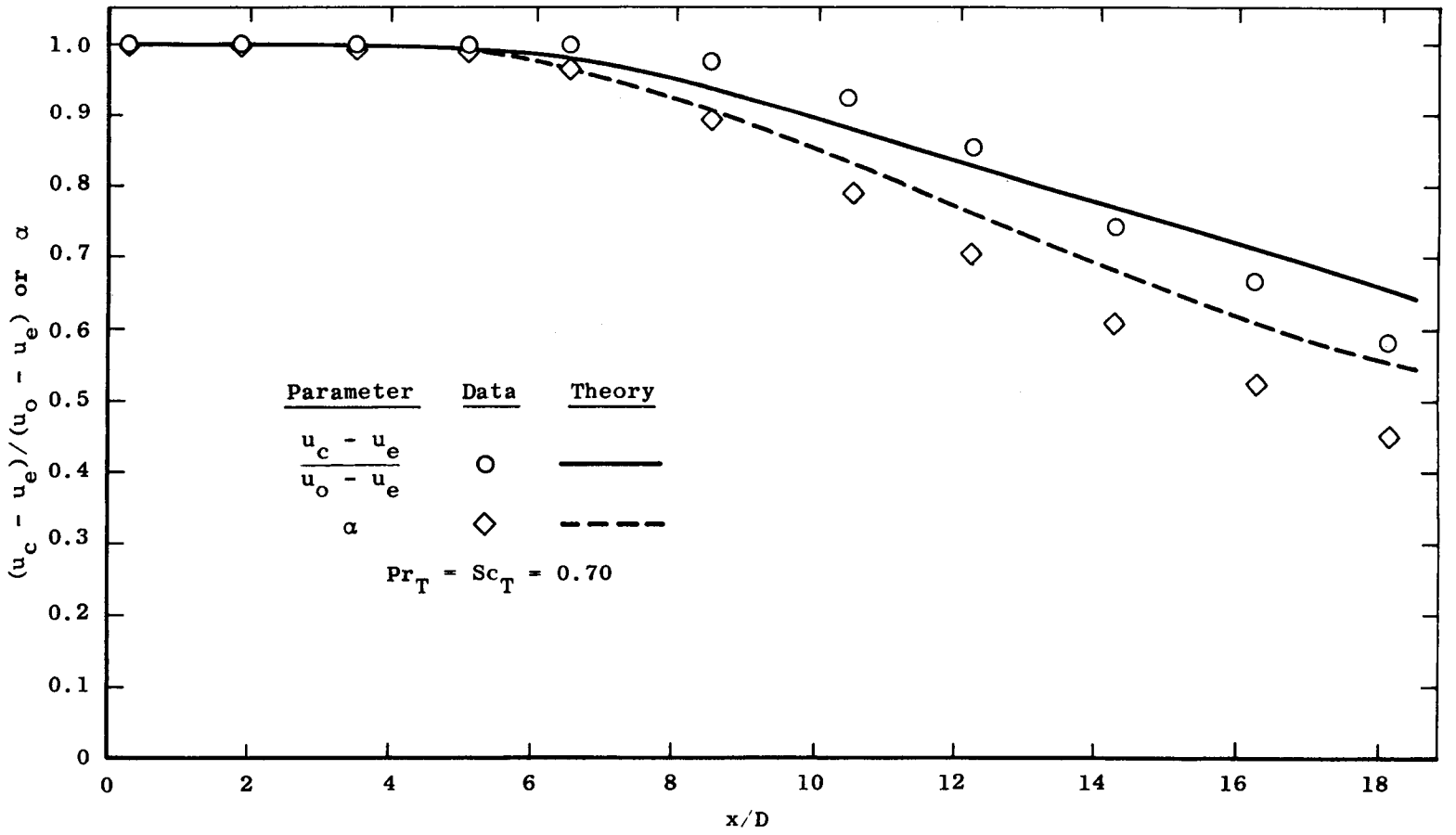

Figure 32.- Comparison of theoretical predictions of center-line velocity and jet species concentration with experimental data for test case 20, coaxial air jets.

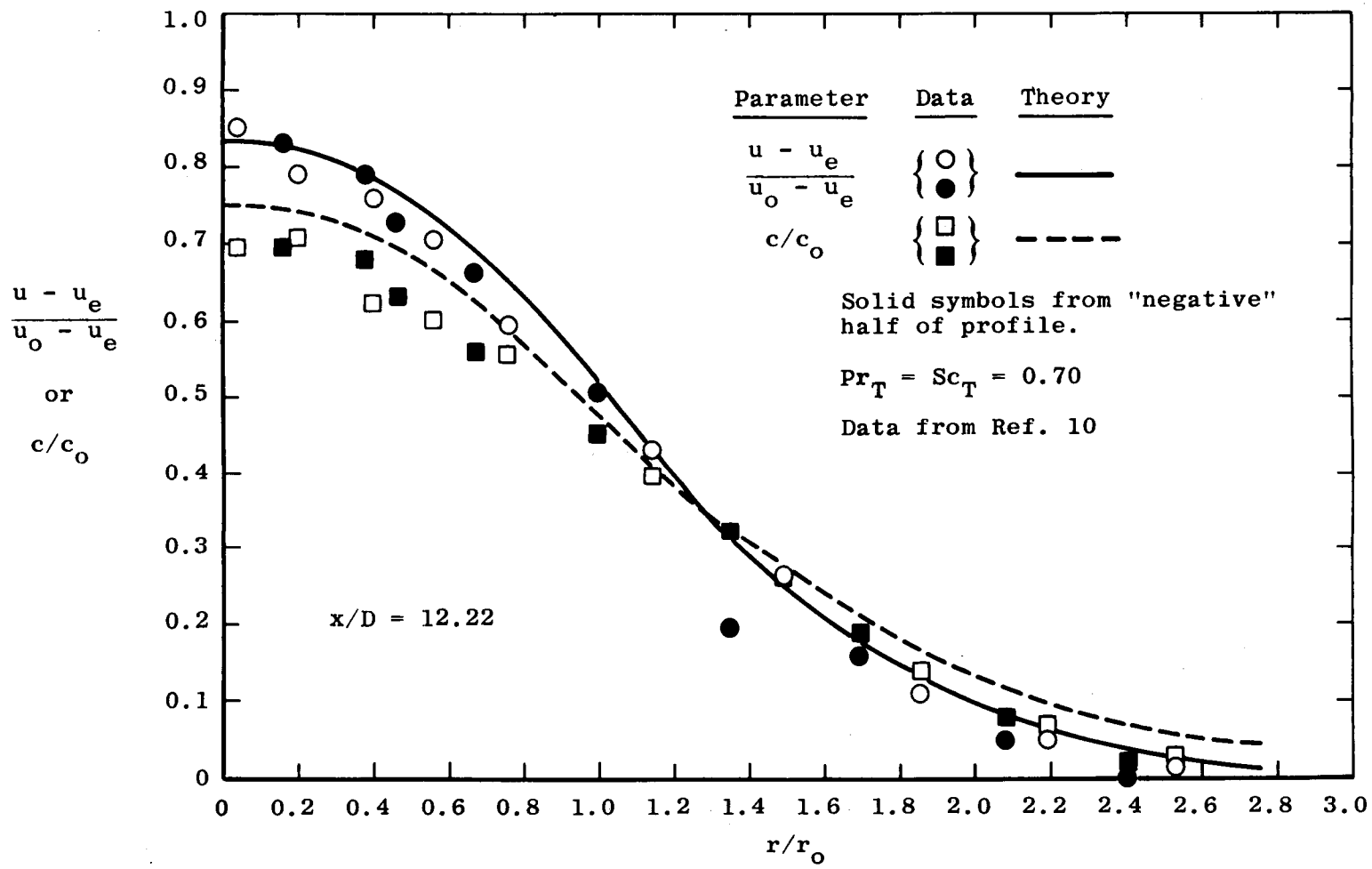

Figure 33.- Comparison of theoretical and experimental profiles for test case 20, coaxial air-air jets with H_2 trace.

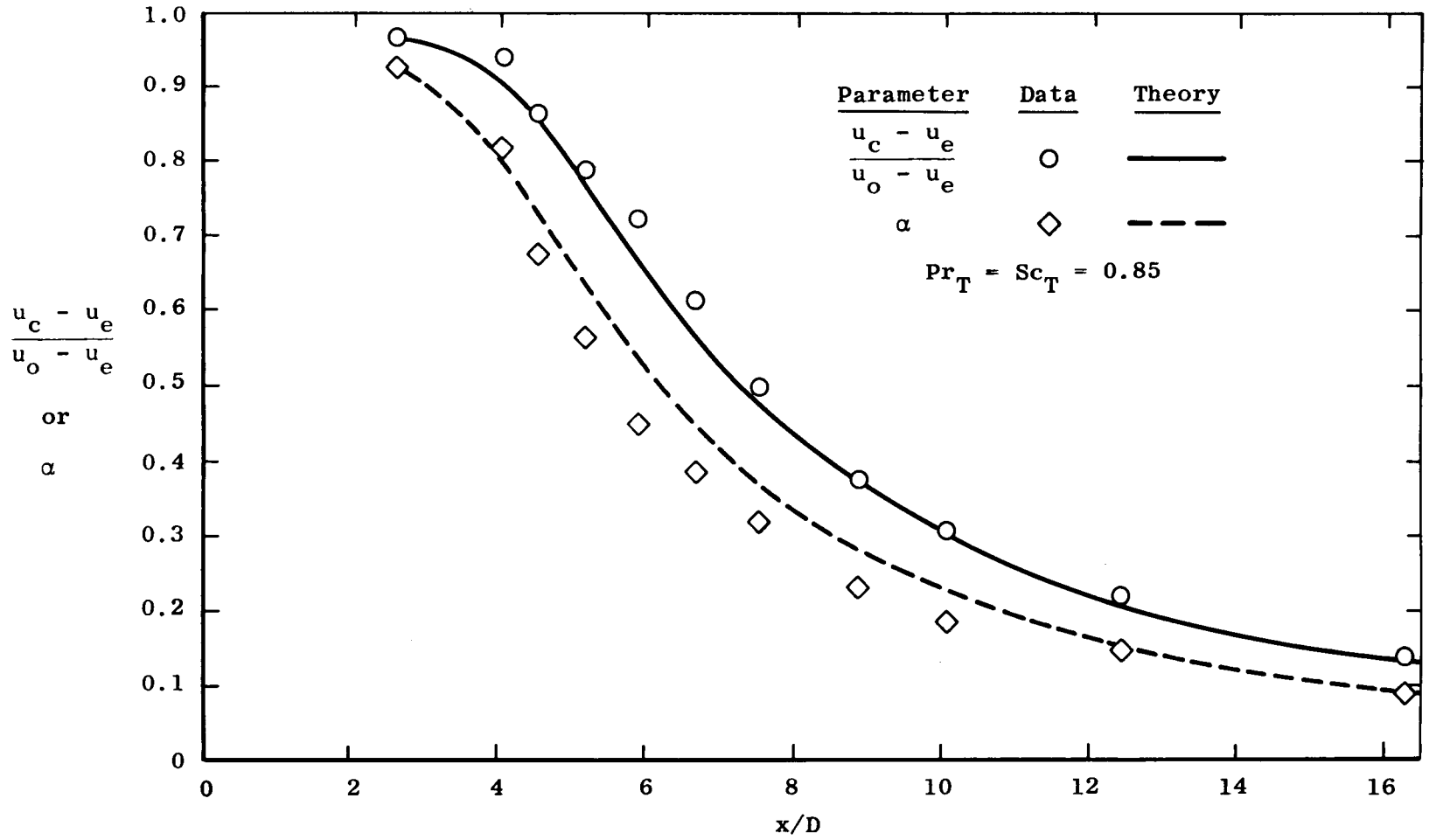

Figure 34.- Comparison of theoretical prediction of center-line velocity and composition decay with experimental data for test case 21, coaxial H_2-air mixing.

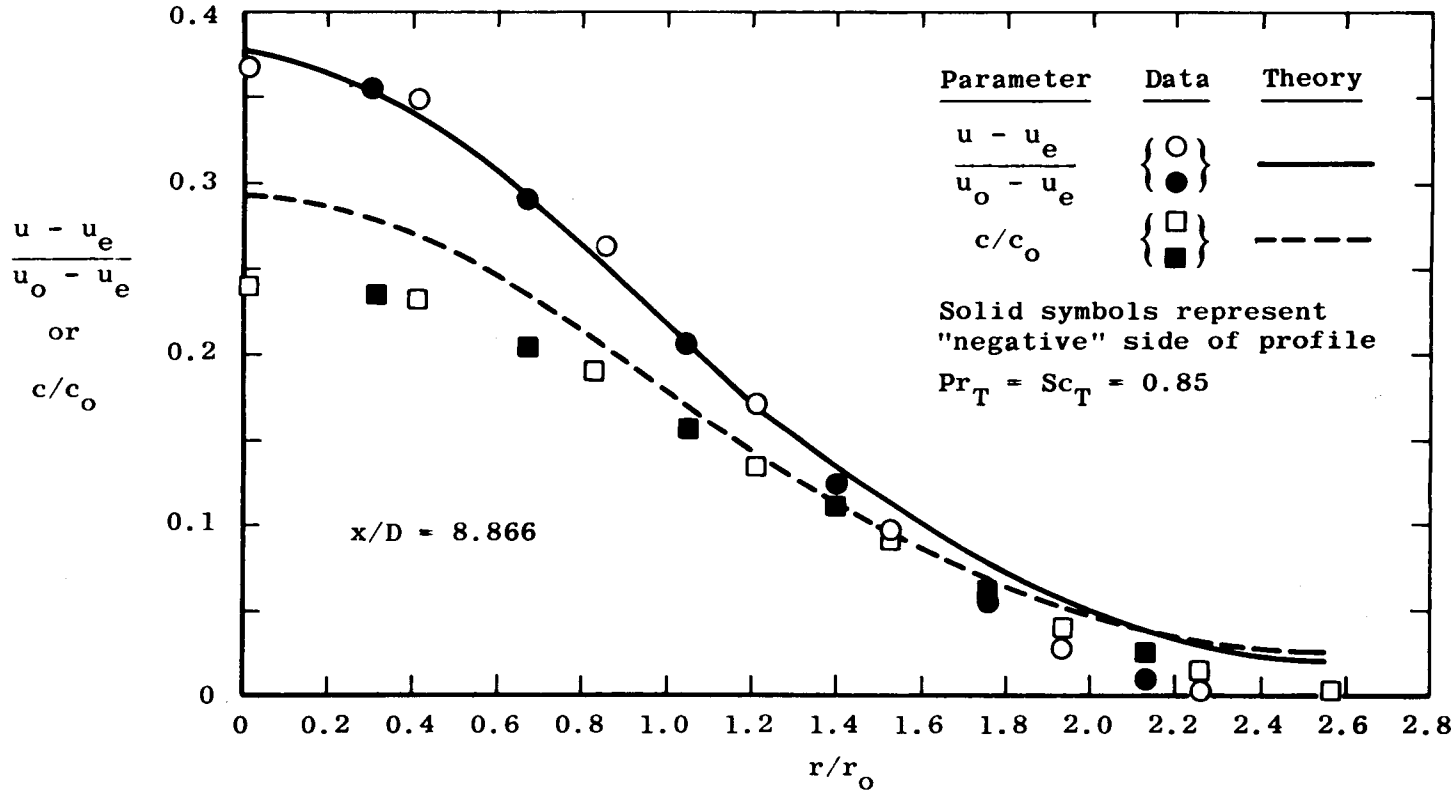

Figure 35.- Comparison of predicted and experimental profiles for test case 21, coaxial H_2-air mixing.

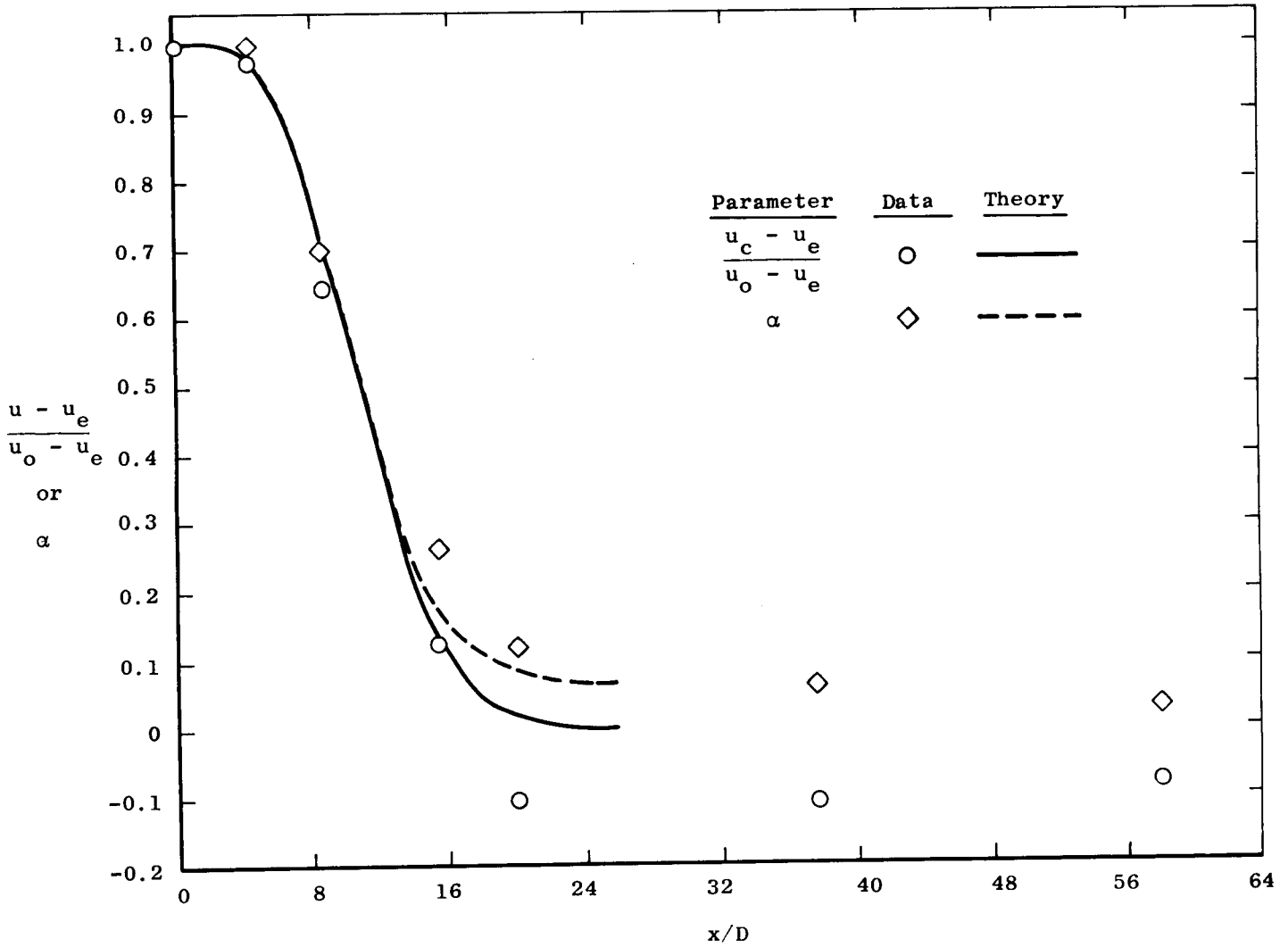

Figure 36.- Comparison of predicted center-line velocity and composition decay with experiment for test case 22, $M_O = 2.50$, H_2-air jets.

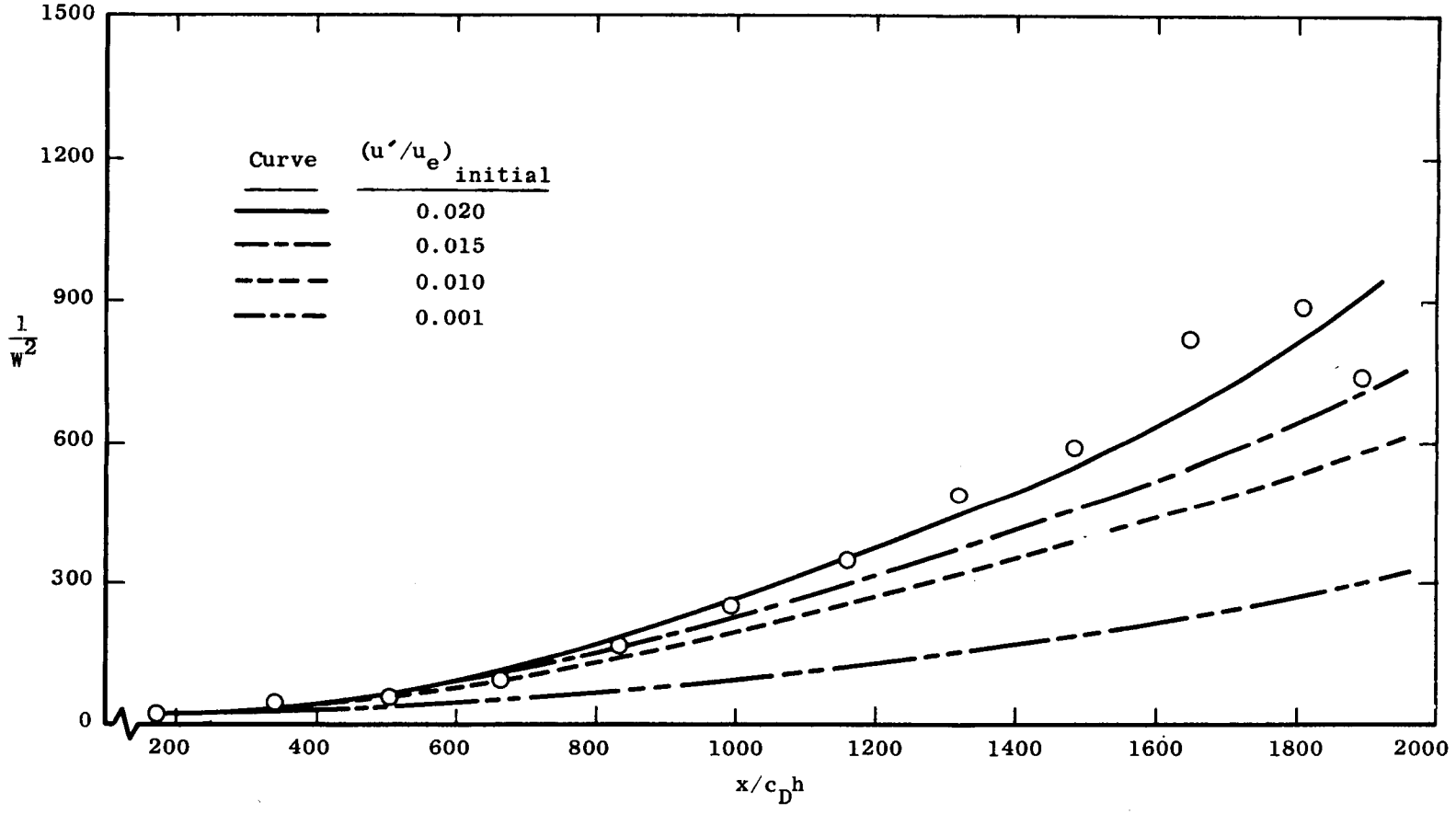

Figure 37.- Comparison of theoretical and experimental distribution of center-line velocity for test case 24, two-dimensional heated wake, $M_e = 2.9$, laminar start.

DISCUSSION

D. M. Bushnell: What has been your experience as far as predicting core length for heterogeneous mixing? You show results which indicate that you are picking up the right core length. I wonder, do you feel confident that this is a feature of your method and that you automatically get this?

P. T. Harsha: I feel confident that I get in the "right ballpark" with the core length. However, I am not overly confident that I can predict core length in every case. The results I show here, if I can use the Maise and McDonald type of start, seem to do quite well, however.

J. M. Eggers: Could you describe your experiences in applying this technique to the reacting flow field for which I understand you have performed at least some preliminary calculations.

P. T. Harsha: The problem with the reacting flow calculation is in general that the density field has an even larger density variation across the shear fields and this tends to create numerical difficulty for me. The results which we have reported using this have not used the a_1 and a_2 models I have described here, but that was only because we were attempting to reproduce some experimental results which were probably in error in any case. I think that the technique as described here can be used for calculations for reacting flows – the only problem being the amount of finesse required to handle large density ratios.

D. B. Spalding: I wonder if you could explain why you say you are using Bradshaw's model. I know that you start off by looking at the equation $\tau = a_1 \rho k$, but no sooner have you got it than you depart from it by saying a_1 must vary. The thing which is queer about the Bradshaw relationship is that it does require that the shear be proportional to the energy, and so you promptly change. Now your old method was to make a_1 proportional to the velocity gradient which immediately gives you an effective viscosity type of relationship. There is a direct proportionality between the shear stress and the velocity gradient. Later on you seem to have done more complicated things. But it seems to me that right from the start you just introduced Bradshaw's hypothesis and then threw it away while retaining the name.

P. T. Harsha: Your comment is well taken. I really meant to say that the hypothesis that I used was originally introduced by Bradshaw but it is necessary to put a lateral variation of a_1 in an axisymmetric flow. I don't believe that Bradshaw has attempted axisymmetric flows.

I. E. Alber: How do you obtain the length scale l_k in your formulation?

P. T. Harsha: The length scale is simply a geometric length scale. In the shear layer region, it is taken to be equal to the distance between the 99- and 1-percent velocity points and in the developed region of a jet it is taken to be twice the half-radius.

I. E. Alber: Also with respect to the two-dimensional mixing layer, I noticed that you find little variation with Mach number as other predictors have found, but with respect to the variation of the spreading parameter σ with the density ratio you find quite a considerable variation. Can you explain that?

P. T. Harsha: No. All I can say is that those were the results that I got. I simply ran the case to see what happened. I have no good explanation for it.

M. V. Morkovin: It seems to me that it would be desirable for you to take a good look at where it comes from because this is the central issue of the density stuff. If there is a clue in the thing it would be nice to know, and if it's a fluke, then it's a fluke, but it seems to me you want to follow up Alber's comment and see where it comes from.

P. T. Harsha: Well I fully agree, and I simply did not have time in preparing for this conference to look at it any more thoroughly than to just run the calculations. But I definitely agree that this is a major problem that must be faced.

Written Comment

S. C. Lee: Referring to the original paper I presented to an AIAA meeting in 1969,[1] I am very glad to see that Dr. Harsha has applied this method to supersonic free mixing problems. However, using several values for one empirical constant is exactly what I wish to eliminate by developing the turbulence kinetic energy method instead of using the simpler eddy viscosity approach. In Harsha's version, the coefficient a_2 (occurring in the dissipation term) is falling into this category. Professor Spalding introduces a dissipation rate equation which is one way to consider the dissipation term of the turbulence kinetic energy equation. I feel the direct approach is to measure the spatial correlations in addition to the Reynolds stresses to obtain a functional relationship of a_2 as I outlined in a paper presented at the 1972 Heat Transfer and Fluid Mechanics Institute.

[1]Lee, S. C.; and Harsha, P. T.: The Use of Turbulent Kinetic Energy in Free Mixing Studies. AIAA Paper No. 69-683, June 1969.

TURBULENT KINETIC ENERGY EQUATION AND FREE MIXING

By P. H. Heck and M. A. Smith
General Electric Company

14

Paper not available for publication

DISCUSSION

W. G. Hill, Jr.: Do you know of any measurements of the jet behind an actual aircraft in flight, where you have a lot of other things going on?

P. H. Heck: I know of tunnel data only, where they have used a scale model of an aircraft and tried to get behind it. Invariably the wake is highly distorted because of the lifting effect of the aircraft.

W. G. Hill: Yes, well that is part of the point. This question is primarily directed towards your comments about IR. In flight, you have a self-propelled body which has a net zero momentum wake. The place where most of the methods seem to have problems is with the wake, where those who do handle the wake use different constants than they do for the jets. Now, for the case where you have a wake and a jet that is essentially one and the same, what do you do?

P. H. Heck: That becomes a rather specialized problem in the IR area, and I don't think that I am able to answer it right here. For one thing, I have to admit that once you get into the particulars of IR, you have to stamp a security classification on everything, and I'll have to leave it out.

S. W. Zelazny: How did you get your initial turbulent energy profiles for cases where they weren't available?

P. H. Heck: We use a flat initial profile, and it has to be an estimate where we are not given information.

S. W. Zelazny: How do you determine the amplitude of the flat profile?

P. H. Heck: In our applications, we have enough data behind our combustion-type engines which give us an empirical model which we can use as a functional start. Otherwise, we have to look at the experiments and, in some cases, if we really want to fit data we have had to look at the experiment very critically and occasionally use trial and error to determine what the initial turbulence should have been. One of the characteristics we have found is that the experiments inherently have had low turbulence and, of course, the real applications have a turbulence of 10 to 20 percent initially.

D. M. Bushnell: I have two questions. First, I don't really understand how we can compute core length for these heterogenous compressible jets but we can't compute developed free shear layers. Is this because these near-field shear layers in the core are low Reynolds numbers or are we adjusting initial turbulence levels?

P. H. Heck: Adjusting initial turbulence levels to make them agree?

D. M. Bushnell: Yes, I just don't understand how we can compute these things and not developed shear layers.

P. H. Heck: The initial turbulence isn't adjusted there. We start with the given quantity and let the flow field develop, and in the parabolic sense we are moving down the axis.

D. M. Bushnell: Maybe it's the low Reynolds number thing catching up with us. The other question is, what about your length scale. You don't tell us what you use, especially in the transition region.

P. H. Heck: The length scale in the mixing layer follows an empirical work by Ollerhead [1] and in the fully developed region it becomes a constant; we have a transition between the two which is an exponential decay. It's empirical, of course.

M. V. Morkovin: Did I understand you correctly that you did use the Spalding model but with different constants?

P. H. Heck: Yes, we retained the constants in the dissipation term and the diffusion term that had been developed previously for boundary-layer work. They work quite well.

M. V. Morkovin: What I am driving at is whether a comparison of your results with those that Professor Spalding presented yesterday (for identical cases) would give us another clue of the sensitivity to changes in the coefficients. You apparently have differences between you, yet you are solving the same problems. Is the assumption correct that there would be some information coming from that?

P. H. Heck: I guess the comparisons of the details would be very valuable. But we have to sit down and see what the minute details are.

D. B. Spalding: It seems to me that what differences appear in the results must lie in the differences in the length scale distributions. That is what we really need to know about. That is where the differences stem from.

P. H. Heck: The length scale is the critical problem in these turbulent kinetic energy solutions.

B. E. Launder: In your presentation, you gave attention to the fact that you had included a correlation between density fluctuations and velocity fluctuation. I'm afraid I missed, however, how you actually approximated this in the model.

P. H. Heck: We used a definition of the turbulent kinetic energy and assumed local isotropy. I will admit that this assumption is going to be very loose in some of these flows with high gradients, both temperature and velocity.

B. E. Launder: I'm not sure that I quite understand what you said there. Are you implying that the correlation between density fluctuations and velocity fluctuations be presumed to be proportional to, say, a mean density gradient times a turbulent viscosity?

---

[1] Ollerhead, J. B.: On the Prediction of Near Field Noise of Supersonic Jets. NASA CR-857, 1967.

P. H. Heck: I'm sorry. In the solution technique, we use the Von Mises transformation. In using the transformation, the transverse momentum mass flux disappears and therefore is not left in the calculation scheme thereafter.

I. E. Alber: I understand, from hearing a talk at a previous AIAA meeting, that your length scale may be a function of the Mach number in some region of the flow. Is that correct?

P. H. Heck: In the initial shear region, the model of Ollerhead includes a term that is related to the jet exit Mach number squared.

I. E. Alber: I think that is quite important for determining that initial shear layer behavior. Also, I would like to comment on an earlier question about the in-flight problem – about the zero momentum wake. Typically, if you have engines mounted on the fuselage, the wakes do not get rolled up in the wing tip vortices, and so you do not have this direct cancellation of the momentum occurring earlier in the jet development. However, if you have the jet engines mounted outboard toward the wing tips, you can get the wakes entrained in the wing tip vortices which carry the induced drag of the aircraft. Then you can get some different momentum effects.

P. H. Heck: I agree.

S. Corrsin: You have assumed a form of the dissipation which is somewhat different from that which other people have assumed. Usually, I think, most of the previous speakers have assumed energy to the three-halves power over a characteristic scale, whereas you have energy over characteristic scale squared so that basically your characteristic length is the Taylor microscale, whereas the other people's characteristic length was basically the integral scale. And I think the shortcoming of this as an engineering technique is that the integral scale tends to be independent of Reynolds number for a given geometry, whereas the microscale tends to be quite sensitive to the Reynolds number for a given geometry. So this might be a more difficult thing to use.

P. H. Heck: We'll look into it.

S. C. Lee: I'm particularly interested in your correlation between acoustic and turbulence energy or turbulent intensity. One of the curves you showed was pressure fluctuations correlated with the intensity U'^2 divided by U^2.

P. H. Heck: The local pressure fluctuations correlated with turbulent intensity, yes.

S. C. Lee: Do you have those two relations directly related with each other? In other words, every time you measure turbulence intensity, can you say that it is also pressure fluctuations?

P. H. Heck: Maestrello's paper [2] showed a relation which included the equation showing the static pressure as a function of turbulence plus a constant times another turbulence term. The constant was arbitrary; not knowing the value of the constant (Maestrello didn't know it either), the assumption that we made at this point was that the constant was zero. Of course, we then took a look at the correlation and it did correlate.

S. C. Lee: So there is a relation but not necessarily a known invariant parameter?

P. H. Heck: Yes, the acoustic relations are much more involved, and that is where you get into the details.

[2] Maestrello, L.; and McDaid, E.: Acoustic Characteristics of a High-Subsonic Jet. AIAA J., vol. 9, no. 6, June 1971, pp. 1058-1066.